Characterization of imatinib as an anti-parkinsonian agent in mouse models of Parkinson's disease

2020

周　禹

CONTENTS

ABSTACT

Parkinson's disease (PD) is caused by a progressive degeneration of nigral dopaminergic neurons leading to striatal dopamine deficiency. In the clinic, administration of dopamine precursor levodopa is the gold standard for the treatment of PD. However, long-term exposure to levodopa often causes side effects, such as levodopa-induced dyskinesia. So development of new therapeutic agents for motor deficits is needed in the treatment of PD. In the last decade, an abnormal activity of the Abelson non-receptor tyrosine kinase (c-Abl) was proved relating to the degeneration of nigral dopaminergic cells in PD. Thereby it has been expected that the inhibition of c-Abl activity would exert anti-parkinsonian effects. Moreover, it has also been reported that a c-Abl inhibitor nilotinib showed acute therapeutic potency on motor symptoms in a PD mouse model, possibly with affecting signaling mechanisms in striatum.

Imatinib, as a c-Abl inhibitor, is currently approved for tumor-related diseases such as human chronic myelogenic leukemia, gastrointestical stromal tumor and Philadelphia chromosome positive acute lymphoblastic leukemia in clinical use. To examine its potential as a PD therapeutic in this study, I evaluated imatinib in two types of PD models of mice: systemically MPTP-induced PD model mice, and unilaterally 6-hyroxydopamine (6-OHDA)-lesioned hemiparkinsonian mice.

When imatinib was systemically administered, the striatum-to-blood concentration ratio of it was about 8%, indicating that peripherally administered imatinib was partially incorporated into the striatum. In MPTP mice, behavioral analysis revealed that a single dose of imatinib (25 mg/kg) could significantly normalized MPTP-induced motor deficits. In western-blot analysis, imatinib significantly reduced the expression of cyclin-dependent kinase 5 (Cdk5) phosphorylated at tyrosine 15 residue (Cdk5-pTyr15) and dopamine- and cAMP-regulated phosphoprotein 32 kDa (DARPP-32) phosphorylated at threonine 75 residue (DARPP-32-pThr75) in striatum, which were increased by MPTP treatment than normal mice. Moreover, I examined the combinatory

effects of imatinib and levodopa. Combination of low doses of imatinib (10 mg/kg) and levodopa (5 mg/kg), which were not effective when solely applied, significantly improved the motor activity of MPTP mice in behavioral tests. In western-blot analysis, the expression of active c-Abl phosphorylated at tyrosine 412 residue (c-Abl-pTyr412), Cdk5-pTyr15 and DARPP-32-pThr75 were also significantly reduced by this combination. These results strongly suggest symptomatic effects of acute imatinib treatment on motor deficits in MPTP mice.

I further evaluated imatinib in 6-OHDA-lesioned hemiparkinsonian mice. Essentially, therapeutic effects of imatinib were also obtained on motor deficits and biochemical changes in this model, which were comparable with the results obtained in MPTP model.

Based on above results, regulating c-Abl/Cdk5/DARPP-32-Thr75 signaling pathway would be important when considering the pathophysiology of motor dysfunctions in PD. I suggest the possibility of a c-Abl inhibitor imatinib as a novel and effective therapeutic agent to treat PD.

KEY WORDS: Parkinson’s disease, c-Abl, striatum, imatinib, Cdk5

ABBREVIATIONS

ANOVA: analysis of variance
ATP: adenosine triphosphate
BBB: blood-brain-barrier
c-Abl: Abelson non-receptor tyrosine kinase
c-Abl-pTyr412: c-Abl phosphorylated at tyrosine 412 residue
Cdk5: cyclin-dependent kinase 5
Cdk5-pTyr15: Cdk5 phosphorylated at tyrosine 15 residue
DA: dopamine
DARPP-32: dopamine- and cyclic AMP-regulated phosphoprotein 32 kDa
DARPP-32-pThr75: DARPP-32 phosphorylated at threonine 75 residue
DARPP-32-pThr34: DARPP-32 phosphorylated at threonine 34 residue
DAT: dopamine transporter
DOPAC: 3, 4-dihydroxyphenylacetic acid
D1R: D1-type dopamine receptor
D2R: D2-type dopamine receptor
ECD: electrochemical detector
ECL: enhanced chemiluminescence
HPLC: high performance liquid chromatography
HVA: homovanillic acid
IMB: imatinib mesylate
i.p.: intraperitoneal
Levodopa: L-3,4-dihydroxyphenylalanine
MPTP: 1-methyl-4-phenyl-1,2,3,6-tetrahydropyridine
6-OHDA: 6-hyroxydopamine
PBS: phosphate-buffered saline
PD: Parkinson’s disease
SDS-PAGE: sodium dodecylsulfate polyacrylamide gel electrophoresis
TH: tyrosine hydroxylase
VMAT2: vesicle monoamine transporter 2

1. INTRODUCTION

Parkinson's disease (PD) is a degenerative disorder of the central nervous system mainly affecting the motor system [1)]. It is caused by a progressive degeneration of nigral dopaminergic neurons leading to striatal dopamine deficiency [2)-3)]. The main pathophysiology of PD is dysfunction of the striatum due to an imbalance between dopamine and glutamate neurotransmission [4)]. In the clinic, administration of dopamine precursor L-3,4-dihydroxyphenylalanine (levodopa) is the gold standard for the treatment of PD. However, long-term exposure to levodopa often causes side effects, such as levodopa-induced dyskinesia and "on-off" periods when levodopa will suddenly and unpredictably start or stop working. Therefore, development of new therapeutic agents for motor deficits and/or progression of neurodegeneration is needed in the treatment of PD.

Abelson non-receptor tyrosine kinase (c-Abl), also known as the Abelson murine leukemia viral oncogene homolog 1, is a member of the Abl family of non-receptor tyrosine kinases [5)]. As c-Abl is highly conserved and ubiquitously expressed in multiple mammalian cellular and subcellular components, it likely plays a role in the regulation of a wide variety of biological processes [6)-7)]. In the brain, under both normal and pathological conditions, c-Abl tyrosine kinase activity is linked to diverse neuronal functions related to cellular signaling [8)-10)], synapse formation [11)-13)], and neurogenesis [14)-16)].

Several studies conducted in a last decade [17)] indicate that dysregulated activity of c-Abl is implicated in the pathogenesis of PD, a neurodegenerative disorder caused by the progressive loss of dopamine producing cells in the substantia nigra [18)-20)]. An increased activity of c-Abl was found in both the substantia nigra and striatum of human and mouse brains under PD conditions [9), 21)-22), 24)]. In PD conditions, over-activation of c-Abl might induce parkin dysfunction [21), 25)-26)], α-synuclein aggregation [23)-24), 27)], and impaired autophagy of toxic elements [28)-30)], leading to the death of the nigral dopaminergic cells. Therefore, systemic administration of c-Abl inhibitors may hold

promise for protection against the degeneration of nigral dopaminergic cells in PD and further anti-parkinsonian effects [23), 31)-34)]. Moreover, it has been demonstrated that c-Abl inhibitors might modulate striatal phosphorylation of specific protein targets at the postsynaptic level, and thereby, exert anti-parkinsonian effects. Abnormal motor behaviors in PD result from striatal dysfunction due to an imbalance between dopamine and glutamate transmission [4), 35)]. A key regulator of the integration of dopamine and glutamate signals is the dopamine- and cAMP-regulated phosphoprotein 32 kDa (DARPP-32) [35)]; corticostriatal glutamate inputs activate cyclin-dependent kinase 5 (Cdk5), which inhibits postsynaptic dopamine signaling by phosphorylating DARPP-32 at threonine 75 residue (DARPP-32-pThr75) [36)]. It had previously been reported that a second generation c-Abl inhibitor, nilotinib (AMN107), normalized motor impairments caused by striatal dopamine deficiency in MPTP mice [37)]. It showed that nilotinib could inhibit the phosphorylation of Cdk5 at tyrosine 15 residue (Cdk5-pTyr15) and phosphorylation of DARPP-32-Thr75 in striatum [37)]. Those data suggests that striatal postsynaptic mechanisms by c-Abl inhibitor represent a symptomatic anti-parkinsonian agent to alleviate motor symptoms.

Imatinib mesylate (STI-571), as a first-generation c-Abl inhibitor, inhibiting the tyrosine kinases c-Abl, v-Abl, Bcr-Abl, c-Kit and platelet-derived growth factor receptor, is currently approved for tumor-related diseases such as human chronic myelogenic leukemia, gastrointestical stromal tumor and Philadelphia chromosome positive acute lymphoblastic leukemia in clinical use [38)-40)]. Imatinib competes with adenosine triphosphate (ATP) antagonistically to inhibit c-Abl activity [41)] and thereby inhibits activation of Cdk5. A previous study reported that striatal effect of imatinib targeted on downstream signaling of D2-type dopamine receptor (D2R), which involved Cdk5 and DARPP-32 as described above, in the post-synaptic medium spiny neurons [42)]. It could possible that imatinib, as well as nilotinib [37)], could alleviate motor symptoms of PD, with avoiding adverse effects of levodopa caused at synaptic levels. Therefore, in this study, I will show the therapeutic effects of imatinib on striatal motor functions

from behavioral analysis, together with biochemical analysis of c-Abl/Cdk5/DARPP-32 signaling pathway in two distinct types of PD model in mice: systemically MPTP-induced PD model mice, and unilaterally 6-hyroxydopamine (6-OHDA)-lesioned hemiparkinsonian mice.

2. MATERIALS AND METHODS

2-1. Experimental Animals

Male C57BL/6 mice (Nihon SLC, Shizuoka, Japan) aged 7-8 weeks were used. The mice were housed under a 12-hour light/dark cycle with *ad libitum* access to food and tap water. All the experimental procedures were approved by the Committee for Animal Experiments of Tokushima University (T28-65, T2019-58).

2-2. MPTP Administration

Mice received intraperitoneal (i.p.) injections of MPTP-HCl (20 mg/kg of free base; Sigma–Aldrich, St Louis, MO, USA) dissolved in 0.9% saline, 4 times per day for one day in 2 hour-intervals [37]. Saline-treated vehicle mice received equivalent volumes of 0.9% saline. A previous study demonstrated that maximal degenerative effects of MPTP on the nigral dopaminergic cells were observed after 3 days of MPTP administration [43]. Therefore I analyzed motor deficits in mice at 3 days after MPTP treatment in this study.

2-3. Levodopa/Benserazide Administration

Mice received a single i.p. injection of levodopa (2.5, 5.0 or 15 mg/kg of free base; Sigma-Aldrich) dissolved in 0.9% saline containing 0.5% carboxymethyl cellulose 3 days after administration of MPTP or saline. Vehicle-treated mice received an equivalent volume of 0.9% saline containing 0.5% carboxymethyl cellulose. They were pre-treated with a single i.p. injection of benserazide HCl (12.5 mg/kg; Sigma–Aldrich) dissolved in 0.9% saline 20 min before administration of levodopa or saline.

2-4. Intraperitoneal Imatinib Administration

Mice received a single i.p. injection of imatinib mesylate (10 or 25 mg/kg; LKT Laboratories, St. Paul, MN, USA) dissolved in 0.9% saline containing 10% dimethyl

sulfoxide 3 days after the administration of MPTP or saline. Vehicle-treated mice received an equivalent volume of 0.9% saline containing 10% dimethyl sulfoxide.

2-5. Nigrostriatal 6-OHDA Lesion

Under anesthesia with N_2O and 2% isoflurane (Sigma-Aldrich, St. Louis, MO, USA), the mice received an i.p. injection of desipramine hydrochloride (an inhibitor of noradrenaline transporter, 1 mg/kg dissolved in 0.9 % saline, Wako, Osaka, Japan) and pargyline hydrochloride (an inhibitor of monoamine oxidase, 0.2 mg/kg dissolved in 0.9% saline, Sigma-Aldrich, St. Louis, MO, USA). I used these inhibitors for up taking 6-OHDA selectively in brain dopaminergic neurons. After 15 min, mice received stereotaxic injections of 6-OHDA HCl (Sigma-Aldrich; 3 μg dissolved in 0.2 μl of 0.9% saline containing 0.2% ascorbic acid) targeted into the medial forebrain bundle (MFB) on the right side. The target coordinates (AP = −1.2, L = +1.1, DV = +5.0) were according to the mouse brain atlas [44]. After a recovery of 2 weeks, the 6-OHDA-lesioned mice, which showed over 80% of the spontaneous ipsilateral rotation and apomorphine (0.5 mg/kg; Sigma-Aldrich) injection-induced contralateral rotation (rotation check), were processed for further placement of programmable intracerebral brain infusion (iCBI) device.

2-6. Implant of iCBI Device and Intrastriatal Imatinib Infusion

The iCBI device equipped with the iPRECIO^{TM} programmable micro infusion pump (Model SMP-300, Primetech Co., Tokyo, Japan) was implanted in the 6-OHDA-lesioned mice under anesthesia with N_2O and 2% isoflurane (Sigma-Aldrich, St. Louis, MO, USA). The infusion cannula was implanted into the dopamine-depleted striatum at the stereotaxic coordinates: AP = +0.3; L = +2.3; and DV = +3.0. Imatinib mesylate (LKT Laboratories) was dissolved in 0.01 M phosphate-buffered saline at pH 7.2 (PBS), and then applied for the infusion pump. Mice received continuous

intrastriatal infusion of imatinib mesylate 0.00078 mg/ml at a flow rate of 0.1 μl/h for the first 5 days (step 1), imatinib mesylate 0.00312 mg/ml at a flow rate of 0.1 μl/h for the next 5 days (step 2), imatinib mesylate 0.0125 mg/ml at a flow rate of 0.1 μl/h for the next 5 days (step 3), imatinib mesylate 0.05 mg/ml at a flow rate of 0.1 μl/h for the next 5 days (step 4), and imatinib mesylate 0.2 mg/ml at a flow rate of 0.1 μl/h for the last 5 days (step 5). In parallel, control mice received continuous intrastriatal infusion of 0.01 M PBS under the same protocol.

2-7. Beam-walking Test

The beam-walking test evaluates motor coordination and balance in rodents. The testing apparatus consists of a rough round horizontal beam (wood, 8-mm-diameter for test trial or 16 mm diameter for training trials, 80 cm long) fixed 60 cm above a countertop, and a dark goal box (15 cm wide, 10 cm long, and 10 cm tall). Mice were trained to traverse the beam without stopping on the way for three consecutive days before MPTP administration. In test trials, mice were made to traverse the beam in the same manner. The traveling time from the start to the 50-cm point was recorded (trials were cut-off at 60 s).

2-8. Rota-rod Test

The rota-rod test evaluates motor coordination and motor learning. The Rota-Rod Treadmill (Constant Speed Model, Ugo Basile, & Varese, Italy) was used. On the day prior to the first training session, mice were habituated to the apparatus for 5 min. Mice were trained to run on the rota-rod for 10 min at 20 rpm without falling, twice a day for three consecutive days before MPTP administration. In the test trials, mice were made to run on rod at 28 rpm (trails were cut-off at 600 s). The latency to fall was recorded.

2-9. Spontaneous Rotation

Spontaneous ipsilateral rotational behaviors were assessed by measuring systemic ipsilateral turns to the 6-OHDA lesion [45]. It was performed at different time points including before and after 6-OHDA lesion, and the last day of imatinib mesylate infusion at different doses (steps) over a period of 44 days. Mice were placed individually into a 1.8-L beaker and the number of ipsilateral and contralateral turns to the 6-OHDA lesion was video-recorded for 30 min. Total turns were summed for both the ipsilateral and contralateral to the 6-OHDA lesion side, the number of ipsilateral turns was calculated as % of the total.

2-10. Analysis of Hind Limb Stepping

Video-based analysis of the hind limb stepping in mice was performed as reported previously [46]. It was performed on the same day as spontaneous rotation. Mice were placed in 600-ml beaker, and the spontaneous steps of their hind limbs were video-recorded from the bottom for 5 min. Each hind limb was counted with a playback speed slowed to 0.3–0.5× using VLC media player. Total hind limb steps were summed for both the ipsilateral and contralateral to the lesion side, and the number of contralateral steps was calculated as % of the total.

2-11. HPLC Analysis

Mice were sacrificed by cervical dislocation 30 min after administration of imatinib mesylate. Striatal tissues and blood were rapidly sampled on ice and kept at - 80°C until use. For the quantification of imatinib, they were homogenized by glycine buffer (0.1 M) at pH 2.75, and imatinib was extracted using an Oasis PRiME Lipophilic Balance extraction cartridge (Waters Corporation, Milford, MA, USA) [47]. HPLC analysis was conducted using an 880-PU Intelligent HPLC pump equipped with an 875- UV Intelligent UV/Vis detector (Jasco, Tokyo, Japan). Chromatographic separation was achieved using a Unison UK-C18 column (100 mm × 4.6 mm, 3μm) at a flow rate of 1

ml/min. The concentration of imatinib was then analyzed using water/methanol/triethylamine (54:45:1) with a pH adjusted to 4.80 ± 0.05 as the mobile phase. The detection wavelength was set to 260 nm, and the injection volume was 50.0 μl. Concentrations of imatinib were expressed as μg/g of total tissue weight or μg/ml of blood volume. The striatal penetration of imatinib was assessed by striatum-to-blood concentration ratios, according to the method described previously [48].

For quantification of striatal dopamine and its metabolites, striatal tissues were homogenized in 500 μl of perchronic acid (50 nM). After adding 400 μl of perchronic acid (50 nM) and 100 μl isoproterenol (as an internal standard substance, 1 μg/ml), homogenates were incubated on ice for 30 min, then centrifuged at 2,500 rpm for 15 min. Extracted samples (50.0 μl) were quantified via HPLC with an electrochemical detector (Eicom, Kyoto, Japan). The concentrations of DA, DOPAC, and HVA were analyzed using octane sulfonic acid (1.064 mM), EDTA-2Na (0.013 mM), 15% methanol, and a 0.1 M sodium citrate-0.1M sodium acetate buffer (pH 3.5) as the mobile phase. Chromatographic separation was achieved using an Eicompak SC-5ODS column (3.0 ∅ × 150 mm). Concentrations of DA, DOPAC, and HVA were expressed as μg/g of total tissue weight [49].

2-12. Western-blot Analysis

Mice were sacrificed by cervical dislocation. Striatal tissues were then quickly sampled and frozen with liquid nitrogen. Striatal tissue samples were prepared according to the Laemmli's method with slight modifications, as in our previous report [37]. Each sample, after being standardized to contain the same amount of protein as other samples, was subjected to 10% sodium-dodecylsulfate polyacrylamide gel electrophoresis, followed by blotting onto a polyvinylidene fluoride membrane. The blotted membranes were then incubated with the desired primary antibodies. Antibodies against TH (1:1000; Millipore, Billerica, MA), DAT (1:1000; Chemicon International, Temecula, CA, USA), VMAT2 (1:500; Santa Cruz Biotechnology, CA, USA),

Cdk5-pTyr15 (1:1000; Santa Cruz Biotechnology, Santa Cruz, CA, USA), Cdk5 (1:1000; Cell Signaling, Danvers, MA, USA), DARPP-32-pThr75 (1:1000; Cell Signaling), DARPP-32-pThr34 (1:1000; Cell Signaling), DARPP-32 (1:1000; Cell Signaling), c-Abl (1:1000; Cell Signaling), and c-Abl-pTyr412 (1:1000; Cell Signaling) were used. Anti-β-actin antibody (1:5000; Sigma-Aldrich) was used for adjustments to ensure that equal amounts of protein were loaded into each well. The bound antibodies were detected by the enhanced chemiluminescence method using horseradish peroxidase-conjugated secondary antibodies. Gel images were captured using a lumino-imaging analyzer LAS-4000 (Fujifilm, Tokyo, Japan). Optical densities were evaluated using a computerized image analysis system (Dolphin-DOC; Kurabo, Osaka, Japan).

2-13. Statistical Analysis

All experimental values were expressed as means ± S.E.M. Statistical significance was evaluated by one-way analysis of variance (ANOVA) followed by the Scheffe *post-hoc* test or two-way ANOVA followed by the Bonferroni *post-hoc* test for pairwise comparisons. The significance level was set at $P < 0.05$. All analysis was conducted in Stat View 5.0 (SAS Institute, Cary, USA).

3. RESULTS

3-1. HPLC quantification of peripherally administered imatinib in naïve mice.

HPLC analysis was performed to quantify various brain regions and blood concentrations of imatinib in naïve mice that received a single i.p. injection of imatinib mesylate (25 mg/kg) 30 min before sacrifice. The concentration of imatinib was calculated as 48.234 ± 2.506 μg/ml in blood (Figure 1A). And that in the striatum was 3.961 ± 0.236 μg/g of tissue weight, in the olfactory bulb was 4.820 ± 0.351 μg/g of tissue weight, in cortex was 3.198 ± 0.046 μg/g of tissue weight, in the hippocampus was 4.806 ± 0.221 μg/g of tissue weight, in the thalamus was 3.472 ± 0.382 μg/g of tissue weight, in the cerebellum was 4.395 ± 0.268 μg/g of tissue weight, and in the spinal cord was 4.827 ± 0.358 μg/g of tissue weight (Figure 1B). Accordingly, the striatum-to-blood concentration ratio of imatinib was 0.083 ± 0.005. Thus, peripherally-administered imatinib was partially passed through blood-brain-barrier (BBB) and incorporated into the striatum, as had been suggested previously [48), 50)].

3-2. A single systemic administration of imatinib normalizes striatal motor behaviors and striatal c-Abl/Cdk5/DARPP-32 signaling cascades in MPTP-treated mice.

3-2-1. Imatinib as well as levodopa normalized MPTP-induced motor deficits.

It has been reported that systemic administration of nilotinib exerted an immediate, therapeutic impact on motor deficits in MPTP-treated mice, as assessed by the beam-walking test, rota-rod test, bar test, horizontal-wire test, and foot-printing test [37)]. In this study, behavioral tests were performed in MPTP-treated mice 30 min after administration of imatinib mesylate or levodopa. In beam-walking test, the traveling time that mice run through the beam was recorded. It was significantly increased in MPTP-treated group, while it was significantly reversed by a single imatinib mesylate injection (25 mg/kg) or levodopa injection (15 mg/kg) compared with vehicle-treated mice (Fig. 2A, $^{*}p < 0.05$).

In rota-rod test, the latency to fall of mice from a rotating rod was measured. It was significantly reduced in MPTP-treated group (Fig. 2B, $^{*}p < 0.05$), while was also sufficiently normalized by a single imatinib mesylate injection (25 mg/kg) or levodopa injection (15 mg/kg) compared with vehicle-treated mice. Thus, a single imatinib mesylate injection (25 mg/kg) has a same therapeutic potency as levodopa (15 mg/kg) in MPTP-treated mice.

3-2-2. Imatinib reduced striatal levels of Cdk5-pTyr15 and DARPP-32-pThr75 in MPTP-treated mice.

It has previously been demonstrated that the immediate therapeutic effect of nilotinib on PD motor symptoms was associated with a normalization of altered striatal Cdk5 and DARPP-32 signals in MPTP-treated mice [37]. Here, I reappraised the effects of c-Abl inhibition on striatal c-Abl/Cdk5/DARPP-32 signaling cascades in MPTP-treated mice 30 min after administration of imatinib mesylate. Western-blot analysis showed MPTP-treated mice significantly increased the striatal levels of Cdk5-pTyr15 (Fig. 3A, $^{*}p < 0.05$) and DARPP-32-pThr75 (Fig. 3B, $^{*}p < 0.05$) compared with vehicle mice, without changing protein expression of total Cdk5 (Fig. 3A), DARPP-32 phosphorylated at threonine 34 residue (DARPP-32-pThr34), nor total DARPP-32 (Fig. 3B). Meanwhile, the MPTP-induced up regulation of striatal levels of Cdk5-pTyr15 and DARPP-32-pThr75 was reversed by the administration of imatinib mesylate (10 mg/kg and 25 mg/kg, Fig. 3A, B, $^{*}p < 0.05$) in a dose-dependent manner.

3-2-3. Imatinib did not affect the striatal TH, DAT and VMAT2 proteins expression in MPTP-treated mice.

With western-blot analysis, protein expression of the striatal presynaptic dopaminergic markers; tyrosine hydroxylase (TH), dopamine transporter (DAT) and vesicle monoamine transporter 2 (VMAT2), was examined. The striatal levels of TH (Fig. 4A, $^{*}p < 0.05$), DAT (Fig. 4B, $^{*}p < 0.05$) and VMAT2 (Fig. 4C, $^{*}p < 0.05$) were

significantly lower in the MPTP-treated mice than in the vehicle-treated mice. Notably, administration of imatinib mesylate had no effect on striatal levels of TH, DAT, or VMAT2 in either vehicle or MPTP-treated mice (Fig. 4A-C).

In addition, HPLC analysis revealed a significant reduction in striatal levels of dopamine (DA; Fig. 5A, $^{*}p < 0.05$), 3,4-dihydroxy-phenylacetic acid (DOPAC; Fig. 5B, $^{*}p < 0.05$) and homovanillic acid (HVA; Fig. 5C, $^{*}p < 0.05$) in MPTP-treated mice as compared to vehicle-treated mice. Striatal DA turnover, as calculated by dividing the total amount of DOPAC and HVA by DA content, was significantly increased (Fig. 5D, $^{*}p < 0.05$) in MPTP-treated mice as compared to vehicle-treated mice. A single administration of imatinib mesylate had no effect on striatal levels of DA, DOPAC, HVA and striatal DA-turnover in either vehicle or MPTP-treated mice (Fig. 5A-D). Thus, the immediate therapeutic effect of imatinib mesylate in MPTP-treated mice depends on postsynaptic, but not presynaptic, striatal mechanisms.

3-3. Combination of lower doses of imatinib and levodopa normalizes striatal motor behaviors and striatal c-Abl/Cdk5/DARPP-32 signaling cascades in MPTP-treated mice.

3-3-1. Combination of lower doses of imatinib and levodopa restored MPTP-induced motor deficits.

Acute single injections of 2.5 or 5.0 mg/kg of levodopa, or 10 mg/kg of imatinib mesylate, had no significant effect on MPTP-induced motor deficits of mice as determined by the beam-walking (Fig. 6A) and rota-rod (Fig. 6B) tests. However, the beam-walking test revealed that administration of levodopa (5.0 mg/kg) combined with imatinib mesylate (10 mg/kg) significantly reduced the traveling time in MPTP-treated mice (Fig. 6A, $^{\#}p < 0.05$). Moreover, the rota-rod test showed that administration of levodopa (2.5 or 5.0 mg/kg) combined with imatinib mesylate (10 mg/kg) significantly increased the latency to fall in MPTP-treated mice (Fig. 6B, $^{\#\#\#}p < 0.001$).

3-3-2. Combination of lower doses of imatinib and levodopa reduced striatal levels of Cdk5-pTyr15, DARPP-32-pThr75, and c-Abl-pTyr412 in MPTP-treated mice.

Western-blot analysis showed that in MPTP-treated mice, an abnormal increase in striatal level of Cdk5-pTyr15 was significantly reduced by administration of imatinib mesylate (10 mg/kg) alone (Figure 7A; $^{\#}P < 0.05$) or imatinib mesylate (10 mg/kg) combined with levodopa (5.0 mg/kg) (Figure 7A; $^{\#\#}P < 0.01$). However, administration of levodopa (5.0 mg/kg) alone had no effect on striatal level of Cdk5-pTyr15. In parallel, an abnormal increase in striatal level of DARPP-32-pThr75 was significantly reduced by administration of imatinib mesylate (10 mg/kg) alone, levodopa (5.0 mg/kg) alone, or imatinib mesylate (10 mg/kg) combined with levodopa (5.0 mg/kg) (Figure 7B; $^{\#}P < 0.05$, $^{\#\#}P < 0.01$). Administration of imatinib mesylate (10 mg/kg) alone, levodopa (5.0 mg/kg) alone, or imatinib mesylate (10 mg/kg) combined with levodopa (5.0 mg/kg) has no effect on striatal level of DARPP-32-pThr34 (Figure 7B). Moreover, striatal level of c-Abl phosphorylated at tyrosine 412 residue (c-Abl-pTyr412), an active form of c-Abl [51)], was significantly reduced by the administration of imatinib mesylate (10 mg/kg) combined with levodopa (5.0 mg/kg) in MPTP-treated mice (Figure 7C; $^{\#}P < 0.05$). Taken together, imatinib showed an inhibitory effect on the c-Abl/Cdk5/DARPP-32-pThr75 signaling pathway in the striatum, as did levodopa.

3-4. Continuous intrastriatal infusion of imatinib normalizes striatal motor deficits and striatal c-Abl/Cdk5/DARPP-32 signaling cascade in 6-OHDA-lesioned mice.

3-4-1. Continuous intrastriatal infusion of imatinib normalized the 6-OHDA-induced motor deficits.

Experimental schedule in this section is shown in Fig. 8A. Fourteen days after 6-OHDA-lesioning targeted into MFB, mice were implanted the iCBI device equipped with iPRECIO^{TM} micro infusion pump, tubing and a stainless steel cannula, targeted into the right side of dopamine-depleted striatum (Fig. 8B, C). The iCBI device allows continuous infusion of drugs at different doses with a programmable, controllable and

implantable system. Fig. 8D showed the image of the right side of striatum after fixation and removal of the cannula. There were abundant Nissl bodies in the right side of striatum, which means it kept normal histology despite of the cannula implanted, except for the cell clusters observed along with the trace of cannula, which is probably representing astrogliosis (Fig.8E).

In the spontaneous rotation, ipsilateral turns as % of total were significantly increased in 6-OHDA-lesioned mice than in naïve mice in both PBS and imatinib groups (Fig. 9A, $^{\$\$\$}p < 0.001$). After the iCBI device was implanted, mice received continuous infusion of PBS or imatinib mesylate into the 6-OHDA-lesioned striatum, as explained in MATERIALS AND METHODS (**2-6**). Intrastriatal infusion of imatinib mesylate significantly reversed this at the dose of 0.0125 mg/ml (step 3; Fig. 9A, $^{***}p < 0.001$), 0.05 mg/ml (step 4; Fig. 9A, $^{***}p < 0.001$), and 0.2 mg/ml (step 5; Fig. 9A, $^{***}p < 0.001$) in a dose-dependent manner.

In the hind limb stepping, contralateral steps as % of the total hind limb steps were significantly reduced by 6-OHDA lesion in both PBS and imatinib groups (Fig. 9B, $^{\$\$\$}p < 0.001$), which were significantly normalized by intrastriatal infusion of imatinib mesylate at the dose of 0.0125 mg/ml (step 3; Fig. 9B, $^{*}p < 0.05$), 0.05 mg/ml (step 4; Fig. 9B, $^{*}p < 0.05$), and 0.2 mg/ml (step 5; Fig. 9A, $^{***}p < 0.001$) in a dose-dependent manner. Taken together, comparing to PBS control, intrastriatal infusion of imatinib mesylate had a significant effect on 6-OHDA-induced motor deficits (Fig. 9A, $^{\#\#\#}p < 0.001$; Fig. 9B $^{\#}p < 0.05$). Thus, PD-like motor deficits in 6-OHDA mice were significantly ameliorated by continuous intrastriatal infusion of imatinib mesylate in a dose-dependent manner.

3-4-2. Continuous intrastriatal infusion of imatinib reduced striatal levels of Cdk5-pTyr15, DARPP-32-pThr75, and c-Abl-pTyr412 in 6-OHDA-lesioned mice.

Western-blot analysis showed the continuous intrastriatal infusion of imatinib mesylate reduced the striatal levels of Cdk5-pTyr15 (Fig. 10A, $^{*}p < 0.05$),

DARPP-32-pThr75 (Fig. 10B, $^{*}p < 0.05$), and c-Abl-pTyr412 (Fig. 10C, $^{*}p < 0.05$) in 6-OHDA-lesioned mice, without changing those of total Cdk5 (Fig. 10A), total DARPP-32 (Fig. 10B), nor total c-Abl (Fig. 10C). Also, DARPP-32-pThr34 but not total DARPP-32 was significantly decreased by 6-OHDA-lesion, which was normalized by continuous intrastriatal infusion of imatinib mesylate (Fig. 11, $^{*}p < 0.05$). Collectively, these results suggest an inhibitory effect of imatinib on the c-Abl/Cdk5/DARPP-32 signaling pathway in the striatum in both MPTP-treated and 6-OHDA-lesioned mice.

4. DISCUSSION

The above results demonstrate that, in two distinct types of mice PD model, imatinib has a therapeutic effect on motor symptoms by systemic administration or by continues intrastriatal infusion. This effect was associated with a normalization of increased levels of striatal Cdk5-pTyr15 and DARPP-32-pThr75 in both PD models, which had previously reported to be regulated as a downstream signal of D2R [42].

In 6-OHDA-lesioned mice, it was also associated with a normalization of 6-OHDA-induced reduction of DARPP-32-pThr34, which is involved in a downstream signaling of D1-type dopamine receptor (D1R) [52]. Previous studies showed that 6-OHDA lesion significantly decreased the striatal D1R expression [53)-54)], which had no change in MPTP-treated mice model [55]. Therefore, 6-OHDA lesion induces the downregulation of D1R/cAMP/PKA signaling activity (Fig. 12), which may lead to the decrease of protein expression of DARPP-32-pThr34.

Acute and systemic administration of imatinib in MPTP mice had no effect on striatal presynaptic dopaminergic markers, as shown in Fig. 4 and 5, strongly suggesting these effects were mediated by postsynaptic manner in striatum. As a major striatal postsynaptic mechanism, dopamine and glutamate signals have been demonstrated to play opposing physiological roles via a positive feedback loop that amplifies their mutually antagonistic actions [35]. Given this, glutamate inputs could activate c-Abl following Cdk5, leading to increased level of DARPP-32-pThr75 and thereby antagonizing striatal dopamine functions [36]. Although the precise mechanism by which c-Abl activity involves interactions between dopamine and glutamate transmission in the striatum remains unknown, land mark reports demonstrated that c-Abl could phosphorylate Cdk5 at tyrosine 15 to increase Cdk5 activity [56)-57)]. Based on a series of studies conducted by our group, including the one presented here, I here hypothesize that c-Abl inhibition exerts symptomatic antiparkinsonian actions via inhibition of Cdk5-pTyr15, thereby, reducing DARPP-32-pThr75 and its downstream signaling pathway, which could be one of a central mechanism underlying motor symptoms in PD

(Fig. 12).

However, the c-Abl inhibitors currently approved for use in clinic have limited BBB penetrance [58], as demonstrated in here for imatinib (Fig. 1), which may limit their clinical utility. In addition, although some c-Abl inhibitors are widely used in the treatment of chronic myelocytic leukemia, the potential risk that they pose for causing serious systemic adverse effects has been reported [17, 59]. In this study, I used the iCBI device makes it possible to deliver imatinib into specific brain regions at very low doses than those by systemic administration, thereby could avoid systemic adverse effects. Collectively, I suggest that c-Abl inhibitors may serve as an alternative agent for attenuating motor symptoms in patients with PD (Fig. 12).

Moreover, some previous evidences showed that c-Abl inhibition may exert disease-modifying effects on PD by playing a protective role against the degeneration of nigral dopaminergic neurons [21-23, 60]. Thus, with applying the iCBI device, future studies examining neuroprotective effects of imatinib on presynaptic nigral dopaminergic neurons in PD model mice would reveal whether it has dual beneficial effects both on PD progression and motor symptoms.

ACKNOWLEDGMENTS

The author would like to thank Professor Koichiro Tsuchiya *(Department of Medical Pharmacology)* and Professor Satoshi Goto *(Department of Neurodegenerative Disorders Research)* for their technical assistance and valuable comments, Associate Professor Jiro Kasahara *(Department of Neurobiology and Therapeutics)* for designing and supervising all the studies, and Mr. Yukio Yamamura and Mr. Masatoshi Ogawa for their collaboration of data analysis with technical support. I thank all members of Department of Neurobiology and Therapeutics, Institute of Biomedical Sciences, Graduate School and Faculty of Pharmaceutical Sciences in Tokushima University, for their kind support for this study.

REFERENCES

1) Santens P., BOON P., VAN ROOST D. and CAEMAERT J. (2003). The pathophysiology of motor symptoms in Parkinson's disease. *Acta Neurol. Belg.*, **103**, 129-134

2) William Dauer, and Serge Przedborski (2003). Parkinson's disease: Mechanisms and Models. *Neuron*, **39**, 889–909. doi: 10.1016/S0896-6273(03)00568-3

3) Julie Lotharius, and Patrik Brundin (2002). Pathogenesis of parkinson's disease: dopamine, vesicles and α-synuclein. *Nature Reviews Neuroscience*, **3**, 932-942. doi: 10.1038/nrn983

4) Olanow, C. W., and Tatton, W. G. (1999). Etiology and pathogenesis of Parkinson's disease. *Annu. Rev. Neurosci.*, **22**, 123-144. doi: 10.1146/annurev.neuro.22.1.123

5) Colicelli, J. (2011). ABL tyrosine kinases: evolution of function, regulation, and specificity. *Sci. Signal*, **3**, re6. doi: 10.1126/scisignal.3139re6

6) Wang, J. Y. (2014). The capable ABL: what is its biological function? *Mol. Cell Biol.*, **34**, 1188-1197. doi: 10.1128/MCB.01454-13

7) Khatri, A., Wang, J., and Pendergast, A. M. (2016). Multifunctional Abl kinases in health and disease. *J. Cell Sci.*, **129**, 9-16. doi: 10.1242/jcs.175521

8) Lee, J. H., Jeong, M. W., Kim, W., Choi, Y. H., and Kim, K. T. (2008). Cooperative roles of c-Abl and Cdk5 in regulation of p53 in response to oxidative stress. *J. Biol. Chem.*, **283**, 19826-19835. doi: 10.1074/jbc.M706201200

9) Ko, H. S., Lee, Y., Shin, J.-H., Karuppagounder, S. S., Gadad, B. S., Koleske, A. J., et al. (2010). Phosphorylation by the c-Abl protein tyrosine kinase inhibits parkin's ubiquitination and protective function. *Proc. Natl. Acad. Sci. U.S.A.*, **107**, 16691-16696. doi: 10.1073/pnas.1006083107

10) Klein, A., Maldonado, C., Vargas, L. M., Gonzalez, M., Robledo, F., Perez de Arce, K., et al. (2011). Oxidative stress activates the c-Abl/p73 proapoptotic pathway in Niemann-Pick type C neurons. *Neurobiol. Dis.*, **41**, 209-218. doi: 10.1016/j.nbd.2010.09.008

11) Finn, A. J., Feng, G., and Pendergast, A. M. (2003). Postsynaptic requirement for Abl kinases in assembly of the neuromuscular junction. *Nat. Neurosci.*, **6**, 717-723. doi: 10.1038/nn1071

12) Perez de Arce, K., Varela-Nallar, L., Farias, O., Cifuentes, A., Bull, P., Couch, B. A., et al. (2010). Synaptic clustering of PSD-95 is regulated by c-Abl through tyrosine phosphorylation. *J. Neurosci.*, **30**, 3728-3738. doi: 10.1523/JNEUROSCI.2024-09.2010

13) Vargas, L. M., Leal, N., Estrada, L. D., González, A., Serrano, F., Araya, K., et al. (2014). EphA4 activation of c-Abl mediates synaptic loss and LTP blockade caused by amyloid-β oligomers. *PLoS ONE*, **9**, e92309. doi: 10.1371/journal.pone.0092309

14) Moresco, E. M., and Koleske, A. J. (2003). Regulation of neuronal morphogenesis and synaptic function by Abl family kinases. *Curr. Opin. Neurobiol.*, **13**, 535-544. doi: 10.1016/j.conb.2003.08.002

15) Woodring, P. J., Hunter, T., and Wang, J. Y. (2003). Regulation of F-actin-dependent processes by the Abl family of tyrosine kinases. *J. Cell Sci.*, **116**, 2613-2626. doi: 10.1242/jcs.00622

16) Schlatterer, S. D., Suh, H. S., Conejero-Goldberg, C., Chen, S., Acker, C. M., Lee, S. C., et al. (2012). Neuronal c-Abl activation leads to induction of cell cycle and interferon signaling pathways. *J. Neuroinflammation*, **9**, 208. doi: 10.1186/1742-2094-9-208

17) Brahmachari, S., Karuppagounder, S. S., Ge, P., Lee, S., Dawson, V. L., Dawson, T. M., et al. (2017). c-Abl and Parkinson's disease: mechanisms and therapeutic potential. *J. Parkinson's Dis.*, **7**, 589-601. doi: 10.3233/JPD-171191

18) Lotharius, J., and Brundin, P. (2002). Pathogenesis of Parkinson's disease: dopamine, vesicles and α-synuclein. *Nat. Rev. Neurosci.*, **3**, 932-942 doi: 10.1038/nrn983

19) Dauer, W., and Przedborski, S. (2003). Parkinson's disease: mechanisms and models. *Neuron*, **39**, 889-909. doi: 10.1016/S0896-6273(03)00568-3

20) Lang, A. E., and Espay, A. J. (2018). Disease modification in Parkinson's disease: current approaches, challenges, and future considerations. *Mov. Disord.*, **00**, 1-18. doi: 10.1002/mds.27360

21) Imam, S. Z., Zhou, Q., Yamamoto, A., Valente, A. J., Ali, S. F., Bains, M., et al. (2011). Novel regulation of parkin function through c-Abl-mediated tyrosine phosphorylation: implications for Parkinson's disease. *J. Neurosci.*, **31**, 157-163. doi: 10.1523/JNEUROSCI.1833-10.2011

22) Imam, S. Z., Trickler, W., Kimura, S., Binienda, Z. K., Paule, M. G., Slikker, W. Jr., et al. (2013). Neuroprotective efficacy of a new brain-penetrating c-Abl inhibitor in a murine Parkinson's disease model. *PLoS ONE*, **8**, e65129. doi: 10.1371/journal.pone.0065129

23) Hebron, M. L., Lonskaya, I., and Moussa, C. E. (2013). Nilotinib reverses loss of dopamine neurons and improves motor behavior via autophagic degradation of α-synuclein in Parkinson's disease models. *Hum. Mol. Genet.*, **22**, 3315-3328. doi: 10.1093/hmg/ddt192

24) Brahmachari, S., Ge, P., Lee, S. H., Kim, D., Karuppagounder, S. S., Kumar, M., et al. (2016). Activation of tyrosine kinase c-Abl contributes to alpha-synuclein-induced neurodegeneration. *J. Clin. Invest.*, **126**, 2970-2988. doi: 10.1172/JCI85456

25) Gonfloni, S., Maiani, E., Di Bartolomeo, C., Diederich, M., and Cesareni, G. (2012). Oxidative Stress, DNA Damage, and c-Abl Signaling: At the Crossroad in Neurodegenerative Diseases? *Int. J. Cell Biol.*, **2012**, 683097. doi: 10.1155/2012/683097

26) Dawson, T. M., and Dawson, V. L. (2014). Parkin plays a role in sporadic Parkinson's disease. *Neurodegener Dis.*, **13**, 69-71. doi: 10.1159/000354307

27) Mahul-Mellier, A. L., Fauvet, B., Gysbers, A., Dikiy, I., Oueslati, A., Georgeon, S., et al. (2014). c-Abl phosphorylates α-synuclein and regulates its degradation: implication for α-synuclein clearance and contribution to the pathogenesis of

Parkinson's disease. *Hum. Mol. Genet.*, **23**, 2858-2879. doi: 10.1093/hmg/ddt674

28) Ertmer, A., Huber, V., Gilch, S., Yoshimori, T., Erfle, V., Duyster, J., et al. (2007). The anticancer drug imatinib induces cellular autophagy. *Leukemia*, **21**, 936-942. doi: 10.1038/sj.leu.2404606

29) Yogalingam, G., and Pendergast, A. M. (2008). Abl kinases regulate autophagy by promoting the trafficking and function of lysosomal components. *J. Biol. Chem.*, **283**, 35941-35953. doi: 10.1074/jbc.M804543200

30) Xu, Y. D., Cui, C., Sun, M.F., Zhu, Y. L., Chu, M., Shi, Y. W., et al. (2017). Neuroprotective effects of loganin on MPTP-Induced Parkinson's disease mice: neurochemistry, glial reaction and autophagy studies. *J. Cell Biochem.*, **118**, 3495-3510. doi: 10.1002/jcb.26010

31) Karuppagounder, S. S., Brahmachari, S., Lee, Y., Dawson, V. L., Dawson, T. M., and Ko, H. S. (2014). The c-Abl inhibitor, Nilotinib, protects dopaminergic neurons in a preclinical animal model of Parkinson's disease. *Sci. Rep.*, **4**, 4874. doi: 10.1038/srep04874

32) Wu, R., Chen, H., Ma, J., He, Q., Huang, Q., Liu, Q., et al. (2016). c-Abl-p38α signaling plays an important role in MPTP-induced neuronal death. *Cell Death Differ.*, **23**, 542-552. doi: 10.1038/cdd.2015.135

33) Zhou, Z.H., Wu, Y.F., Wang, X.M., and Han, Y.Z. (2017). The c-Abl inhibitor in Parkinson disease. *Neurol. Sci.*, **38**, 547-552. doi: 10.1007/s10072-016-2808-2

34) Abushouk, A.I., Negida, A., Elshenawy, R.A., Zein, H., Hammad, A.M., Menshawy, A.,et al. (2018). c-Abl inhibition; a novel therapeutic target for Parkinson's disease. *CNS Neurol. Disord. Drug Targets.*, **17**, 14-21. doi: 10.2174/1871527316666170602101538

35) Greengard, P. (2001). The neurobiology of slow synaptic transmission. *Science*, **294**, 1024-1030. doi: 10.1126/science.294.5544.1024

36) Bibb, J. A., Snyder, G. L., Nishi, A., Yan, Z., Meijer, L., Fienberg, A. A., et al. (1999). Phosphorylation of DARPP-32 by Cdk5 modulates dopamine signaling in

neurons. *Nature*, **402**, 669-671. doi: 10.1038/45251

37) Tanabe, A., Yamamura, Y., Kasahara, J., Morigaki, R., Kaji, R., and Goto, S. (2014). A novel tyrosine kinase inhibitor AMN107 (nilotinib) normalizes striatal motor behaviors in a mouse model of Parkinson's disease. *Front. Cell Neurosci.*, **8**, 50. doi: 10.3389/fncel.2014.00050

38) Ottman, O. G., Pfeifer, H. (2009). First-line treatment of Philadelphia chromosome-positive acute lymphoblastic leukemia in adults. *Curr. Opin. Oncol.*, **21**, S43-46. doi: 10.1097/01.cco.0000357476.43164.6b

39) Efficace, F., Cardoni, A., Cottone, F., Vignetti, M., Mandelli, F. (2013). Tyrosine-kinase inhibitors and patient-reported outcome in chronic myeloid leukemia: a systematic review. *Leuk. Res.*, **37**, 206-213. doi: 10.1016/j.leukres.2012.10.021

40) Patel, S. (2013). Long-term efficacy of imatinib for treatment of metastatic GIST. *Cancer Chemother. Pharmacol.*, **72**, 277-286. doi: 10.1007/s00280-013-2135-8

41) Gambacorti-Passerini, C., le, Coutre, P., Mologni, L., Fanelli, M., Bertazzoli, C., Marchesi, E., Di, Nicola, M., Biondi, A., Corneo, G. M., Belotti, D., Pogliani, E., Lydon, N. B. (1997). Inhibition of the ABL kinase activity blocks the proliferation of BCR/ABL+ leukemic cells and induces apoptosis. *Blood Cells Mol. Dis.*, **23**, 380-394. doi: 10.1006/bcmd.1997.0155

42) Yamamura, Y., Morigaki, R., Kasahara, J., Yokoyama, H., Tanabe, A., Okita, S., et al. (2013). Dopamine signaling negatively regulates striatal phosphorylation of Cdk5 at tyrosine 15 in mice. *Front. Cell Neurosci.*, **7**, 12. doi: 10.3389/fncel.2013.00012

43) Aoki, E., Yano, R., Yokoyama, H., Kato, H., and Araki, T. (2009). Role of nuclear transcription factor kappa B (NF-kappaB) for MPTP (1-methyl-4-phenyl-1,2,3,6-tetrahydropyridine)-induced apoptosis in nigral neurons of mice. *Exp. Mol. Pathol.*, **86**, 57–64. doi: 10.1016/j.yexmp.2008.10.004

44) Paxinos G, Franklin KBJ. (2001). *The Mouse Brain in Stereotaxic Coordinates*, 2 ed.

San Diego, CA: Academic Press

45) Boix J, Padel T, Paul G. (2015). A partial lesion model of Parkinson's disease in mice – characterization of a 6-OHDA-induced medial forebrain bundle lesion. *Behav Brain Res*., **284**, 196–206. doi: 10.1016/j.bbr.2015.01.053

46) Ogawa M, Zhou Y, Tsuji R, Goto S, Kasahara J. (2019). Video-based assessments of the hind limb stepping in a mouse model of hemi-parkinsonism. *Neurosci Res.*, **19**, S0168-0102, 30143-9. doi: 10.1016/j.neures.2019.05.002.

47) Miura, M., Takahashi, N., and Sawada, K. (2011). Quantitative determination of imatinib mesylate in human plasma with high-performance liquid chromatography and ultraviolet detection. *J. Chromatogr. Sci.*, **49**, 412-415. doi: 10.1093/chromsci/49.5.412

48) Bihorel S, Camenisch G, Lemaire M, Scherrmann JM. (2007). Modulation of the brain distribution of imatinib mesylate and its metabolites in mice by valspodar, zosuquidar and elacridar. *Pharm. Res.*, **24**, 1720-1728. doi: 10.1007/s11095-007-9278-4

49) Kadoguchi, N., Okabe, S., Yamamura, Y., Shono, M., Fukano, T., Tanabe, A., et al. (2014). Mirtazapine has a therapeutic potency in 1-methyl-4-phenyl-1, 2, 3, 6-tetrahydropyridine (MPTP)-induced mice model of Parkinson's disease. *BMC Neurosci.*, 15:79. doi: 10.1186/1471-2202-15-79

50) Breedveld, P., Pluim, D., Cipriani, G., Wielinga, P., van Tellingen, O., Schinkel, A. H., et al. (2005). The effect of Bcrp1 (Abcg2) on the *in vivo* pharmacokinetics and brain penetration of imatinib mesylate (Gleevec): implications for the use of breast cancer resistance protein and P-glycoprotein inhibitors to enable the brain penetration of imatinib mesylate in patients. *Cancer Res.*, **65**, 2577-2582. doi: 10.1158/0008-5472

51) Brasher, B. B., and Van Etten, R. A. (2000). c-Abl has high intrinsic tyrosine kinase activity that is stimulated by mutation of the Src homology 3 domain and by autophosphorylation at two distinct regulatory tyrosines. *J. Biol. Chem.*, **275**,

35631-35637. doi: 10.1074/jbc.M005401200

52) Kuroiwa M., Bateup H.S., Shuto T., Higashi H., Tanaka M., and Nishi A. (2008). Regulation of DARPP-32 phosphorylation by three distinct dopamine D1-like receptor signaling pathways in the neostriatum. *J Neurochem.*, **107**, 1014-26. doi: 10.1111/j.1471-4159.2008.05702.x

53) Mishra A., Singh S., Tiwari V., Chaturvedi S., Wahajuddin M., and Shukla S. (2019). Dopamine receptor activation mitigates mitochondrial dysfunction and oxidative stress to enhance dopaminergic neurogenesis in 6-OHDA lesioned rats: A role of Wnt signalling. *Neurochem Int.*, **129**, 104463. doi: 10.1016/j.neuint.2019.104463

54) Rui G., Guangjian Z., Yong W., Jie F., Yanchao C., Xi J., et al. (2013) . High frequency electro-acupuncture enhances striatum DAT and D1 receptor expression, but decreases D2 receptor level in 6-OHDA lesioned rats. *Behav Brain Res.*, **15**, 237:263-9. doi: 10.1016/j.bbr.2012.09.047

55) Vučković M.G., Li Q., Fisher B., Nacca A., Leahy R.M., Walsh J.P., et al. (2010). Exercise elevates dopamine D2 receptor in a mouse model of Parkinson's disease: in vivo imaging with [^{18}F]fallypride. *Mov Disord.*, **25**, 2777-84. doi: 10.1002/mds.23407

56) Zukerberg, L. R., Patrick, G. N., Nikolic, M., Humbert, S., Wu, C. L., Lanier, L. M., et al. (2000). Cables links Cdk5 and c-Abl and facilitates Cdk5 tyrosine phosphorylation, kinase upregulation, and neurite outgrowth. *Neuron*, **26**, 633–646. doi: 10.1016/S0896-6273(00)81200-3

57) Zhang, B., Tan, V. B., Lim, K. M., and Tay, T. E. (2007). The activation and inhibition of cyclin-dependent kinase-5 by phosphorylation. *Biochemistry*, **46**, 10841-10851. doi: 10.1021/bi700890t

58) Lindholm, D., Pham, D. D., Cascone, A., Eriksson, O., Wennerberg, K., and Saarma, M. (2016). c-Abl Inhibitors enable insights into the pathophysiology and neuroprotection in Parkinson’s disease. *Front. Aging Neurosci.*, **8**, 254. doi:

10.3389/fnagi.2016.00254

59) Arora, A., and Scholar, E. M. (2005). Role of tyrosine kinase inhibitors in cancer therapy. *J. Pharmacol. Exp. Ther.*, **315**, 971-979. doi: 10.1124/jpet.105.084145

60) Hebron, M. L., Lonskaya, I., and Moussa, C. E. (2013). Tyrosine kinase inhibition facilitates autophagic SNCA/α-synuclein clearance. *Autophagy*, **9**, 1249-1250. doi: 10.4161/auto.25368

FIGURE LEGENDS

Figure 1. HPLC quantification of peripherally administered imatinib in naïve mice. HPLC analysis was performed to quantify concentrations of imatinib in the blood (n = 5), striatum (n = 4), olfactory bulb (n = 4), cortex (n = 5), hippocampus (n = 4), thamalus (n = 4), cerebellum (n = 4), and spinal cord (n = 4) of naïve mice that received single i.p. injection of imatinib mesylate (25 mg/kg) 30 min before sacrifice. Values are expressed as means ± S.E.M.

Figure 2. Symptomatic anti-parkinsonian effects of imatinib or levodopa in MPTP-treated mice. Behavioral tests were carried out in vehicle or MPTP-treated mice 30 min after single i.p. injection of imatinib or levodopa.

(A) The beam-walking test for examining the effects of administration of imatinib mesylate (25 mg/kg) or levodopa (15 mg/kg). Values are means ± S.E.M (n = 5-21). $^{*}P < 0.05$ versus vehicle-treated mice; one-way ANOVA [$F_{(5, 77)} = 11.265$] followed by the Scheffe *post-hoc* test.

(B) The rota-rod test for examining the effects of imatinib mesylate (25 mg/kg) or levodopa (15 mg/kg) administration. Values are means ± S.E.M (n = 8-21). $^{*}P < 0.05$ versus vehicle-treated mice; one-way ANOVA [$F_{(5, 80)} = 7.710$] followed by the Scheffe *post-hoc* test.

Figure 3. Western-blot analysis of the striatal levels of Cdk5-pTyr15, Cdk5, DARPP-32-pThr75, DARPP-32-pThr34, and DARPP-32 in vehicle or MPTP-treated mice 30 min after single i.p. injection of imatinib.

(A) Western-blot analysis of the striatal levels of Cdk5-pTyr15 and Cdk5. Values are means ± S.E.M (n = 4-5). $^{*}P < 0.05$ versus vehicle-treated mice; one-way ANOVA [$F_{\text{Cdk5-pTyr15 (4, 19)}} = 50.391$, $F_{\text{Cdk5 (4, 19)}} = 1.413$] followed by the Scheffe *post-hoc* test. IMB (10), imatinib mesylate (10 mg/kg); IMB (25), imatinib mesylate (25 mg/kg).

(B) Western-blot analysis of the striatal levels of DARPP-32-pThr75,

DARPP-32-pThr34, and DARPP-32. Values are means ± S.E.M (n = 4-5). $^{*}P < 0.05$ versus vehicle-treated mice; one-way ANOVA [$F_{\text{DARPP-32-pThr75 (4, 19)}} = 35.089$, $F_{\text{DARPP-32-pThr34 (4, 19)}} = 0.711$, $F_{\text{DARPP-32 (4, 19)}} = 0.293$] followed by the Scheffe *post-hoc* test. IMB (10), imatinib mesylate (10 mg/kg); IMB (25), imatinib mesylate (25 mg/kg).

Figure 4. Effects of imatinib on striatal presynaptic dopaminergic markers in MPTP-treated mice. Western-blot analysis of striatal levels of TH, DAT, and VMAT2 were carried out from vehicle or MPTP-treated mice 30 min after single i.p. injection of imatinib mesylate (10 or 25 mg/kg). $^{*}P < 0.05$ versus vehicle-treated mice; one-way ANOVA [$F_{\text{TH (4, 19)}} = 107.43$, $F_{\text{DAT (4, 19)}} = 21.749$, $F_{\text{VMAT2 (4, 19)}} = 20.615$] followed by the Scheffe *post-hoc* test. IMB (10), imatinib mesylate (10 mg/kg); IMB (25), imatinib mesylate (25 mg/kg).

Figure 5. HPLC analysis of striatal levels of DA (A), DOPAC (B), HVA (C), and DA-turnover, which represents a net dopamine usage in striatum with (DOPAC + HVA)/DA (D). Values are expressed as means (μg/g tissue) ± S.E.M. (n = 4-5). $^{*}P < 0.05$ versus vehicle-treated mice; one-way ANOVA [$F_{\text{DA (4, 19)}} = 34.526$, $F_{\text{DOPAC (4, 19)}} = 15.383$, $F_{\text{HVA (4, 19)}} = 16.078$, $F_{\text{DA-turnover (4, 19)}} = 10.355$] followed by the Scheffe *post-hoc* test. IMB (10), imatinib mesylate (10 mg/kg); IMB (25), imatinib mesylate (25 mg/kg).

Figure 6. Symptomatic anti-parkinsonian effects with combining lower doses of imatinib and levodopa in MPTP-treated mice. Behavioral tests were carried out in vehicle or MPTP-treated mice 30 min after single i.p. injection of imatinib and/or levodopa.

(A) The beam-walking test for examining the effects of imatinib mesylate (10 mg/kg) and/or levodopa (2.5 or 5.0 mg/kg) administration. Values are means ± S.E.M (n = 10-11). $^{\#}P < 0.05$ versus MPTP-treated mice; one-way ANOVA [$F_{(5, 55)} = 4.177$] followed by the Scheffe *post-hoc* test.

(B) The rota-rod test for examining the effects of imatinib mesylate (10 mg/kg) and/or levodopa (2.5 or 5.0 mg/kg) administration. Values are means ± SEM (n =10-11). $^{###}P <$ 0.001 versus MPTP-treated mice group; one-way ANOVA [$F_{(5, 55)} = 8.283$] followed by the Scheffe *post-hoc* test.

Figure 7. Western-blot analysis in MPTP-treated mice 30 min after single i.p. injection of imatinib and/or levodopa.

(A) Western-blot analysis of the striatal levels of Cdk5-pTyr15 and Cdk5. Values are expressed as means ± S.E.M. (n = 5-10). $^{\#}P < 0.05$ or $^{\#\#}P < 0.01$ versus MPTP-treated mice. One-way ANOVA [$F_{\text{Cdk5-pTyr15 (3, 31)}} = 6.039$, $F_{\text{Cdk5 (3, 17)}} = 0.258$] followed by the Scheffe *post-hoc* test.

(B) Western-blot analysis of the striatal levels of DARPP-32-pThr75, DARPP-32-pThr34, and DARPP-32. Values are expressed as means ± S.E.M. (n = 4-10). $^{\#}P < 0.05$ or $^{\#\#}P < 0.01$ versus MPTP-treated mice. One-way ANOVA [$F_{\text{DARPP-32-pThr75 (3, 29)}} = 5.529$, $F_{\text{DARPP-32-pThr34 (3, 16)}} = 1.257$, $F_{\text{DARPP-32 (3, 16)}} = 2.886$] followed by the Scheffe *post-hoc* test.

(C) Western-blot analysis of the striatal levels of c-Abl-pTyr412 and c-Abl. Values are expressed as means ± S.E.M. (n = 8-11). $^{\#}P < 0.05$ compared with MPTP-treated mice; One-way ANOVA [$F_{\text{c-Abl-pTyr412 (3, 34)}} = 5.820$, $F_{\text{c-Abl (3, 29)}} = 0.240$] followed by the Scheffe *post-hoc* test.

Figure 8. Experimental schedule and implant of the iCBI device with striatal tissue images in mice.

(A) 6-OHDA-lesioned mice were implanted with the iCBI device equipped with iPRECIO^{TM} micro infusion pump. After a recovery of 3 days, mice received continuous intrastriatal infusion of imatinib mesylate 0.00078 mg/ml at a flow rate of 0.1 μl/h for the first 5 days (step 1), imatinib mesylate 0.00312 mg/ml at a flow rate of 0.1 μl/h for the next 5 days (step 2), imatinib mesylate 0.0125 mg/ml at a flow rate of 0.1 μl/h for

the next 5 days (step 3), imatinib mesylate 0.05 mg/ml at a flow rate of 0.1 μl/h for the next 5 days (step 4), and imatinib mesylate 0.2 mg/ml at a flow rate of 0.1 μl/h for the last 5 days (step 5). In parallel, the PBS-infusion mice received 0.01 M PBS under the same protocol. At the end of infusion, mice were dissected and striatal tissues were used for western-blot analysis.

(B) The infusion pump and tubing connected with a stainless steel cannula were implanted under the skin, targeted into the right side of dopamine-depleted striatum of mice.

(C) A schematic image of the infusion cannula implanted into the right side of dopamine-depleted striatum.

(D) An optical microscopic image of the right side of striatum after fixation and removal of the cannula. Scale bar shows 0.5 mm.

(E) A Nissl staining image of the right side of striatum after fixation and removal of the cannula. Scale bar shows 100 μm.

Figure 9. Symptomatic anti-parkinsonian effects of imatinib in 6-OHDA-lesioned mice. Spontaneous rotation and hind limb steps were analyzed after continuous intrastriatal infusion of imatinib.

(A) Spontaneous rotations ipsilateral to the 6-OHDA-lesioned side shown as % of total. $^{\$\$\$}p < 0.001$ compared with vehicle-treated mice; $^{***}p < 0.001$ compared with 6-OHDA-lesioned mice; $^{\#\#\#}p < 0.001$ compared with PBS control; two-way ANOVA ($F_{(group)\ 1} = 92.505$, $F_{(step)\ 6} = 103.491$, $F_{(group*step)\ 6,\ 72} = 11.331$) followed by Bonferroni *post-hoc* test. PBS, 0.01 M phosphate-buffered saline; IMB, imatinib mesylate.

(B) Spontaneous contralateral hind limb steps as % of total. Values are expressed as means ± S.E.M. (n = 5). $^{\$\$\$}p < 0.001$ compared with vehicle-treated mice; $^{*}p < 0.05$ or $^{***}p < 0.001$ compared with 6-OHDA-lesioned mice; $^{\#}p < 0.05$ compared with PBS control at step 5; two-way ANOVA ($F_{(group)\ 1} = 6.443$, $F_{(step)\ 6} = 5.947$, $F_{(group*step)\ 6,\ 48} = 1.613$) followed by Bonferroni *post-hoc* test. PBS, 0.01 M phosphate-buffered saline;

IMB, imatinib mesylate.

Figure 10. Western-blot analysis in 6-OHDA-lesioned mice after continuous intrastriatal infusion of imatinib.

(A) Western-blot analysis of the striatal levels of Cdk5-pTyr15 and Cdk5. Values are expressed as means ± S.E.M. (n = 5-6). $^{*}p < 0.05$ followed by paired *t*-test. PBS, 0.01 M phosphate-buffered saline; IMB, imatinib mesylate; con, contralateral striatum; ips, ipsilateral striatum.

(B) Western-blot analysis of the striatal levels of DARPP-32-pThr75 and DARPP-32. Values are expressed as means ± S.E.M. (n = 5-6). $^{**}p < 0.01$ followed by paired *t*-test. PBS, 0.01 M phosphate-buffered saline; IMB, imatinib mesylate; con, contralateral striatum; ips, ipsilateral striatum.

(C) Western-blot analyses of the striatal levels of c-Abl-pTyr412 and c-Abl. Values are expressed as means ± S.E.M. (n = 5-7). $^{*}p < 0.05$ followed by paired *t*-test. PBS, 0.01 M phosphate-buffered saline; IMB, imatinib mesylate; con, contralateral striatum; ips, ipsilateral striatum.

Figure 11. Western-blot analysis of the striatal level of DARPP-32-pThr34 in 6-OHDA-lesioned mice after continuous intrastriatal infusion of imatinib. Values are expressed as means ± S.E.M. (n = 6-7). $^{*}p < 0.05$ followed by paired *t*-test. PBS, 0.01 M phosphate-buffered saline; IMB, imatinib mesylate; con, contralateral striatum; ips, ipsilateral striatum.

Figure 12. A hypothetical scheme showing symptomatic anti-parkinsonian effects of c-Abl inhibitors. Depicted are the possible roles of c-Abl inhibitors at postsynaptic level in the striatum. In the postsynaptic medium spiny neurons, dopamine deficiency may induce c-Abl activation to increase phosphorylation of Cdk5-pTyr15 and DARPP-32-pTyr75, resulting in an increased activity of the Cdk5/DARPP32-pThr75

pathway, which leads to parkinsonian symptoms. Thus, c-Abl inhibitors may exert symptomatic anti-parkinsonian effects at the postsynaptic level. PD, Parkinson's disease; D1R, D1-type dopamine receptor; D2R; D2-type dopamine receptor; Cdk5-pTyr15, Cdk5 with tyrosine 15 phosphorylation; T34, Threonine 34; T75, Threonine 75.

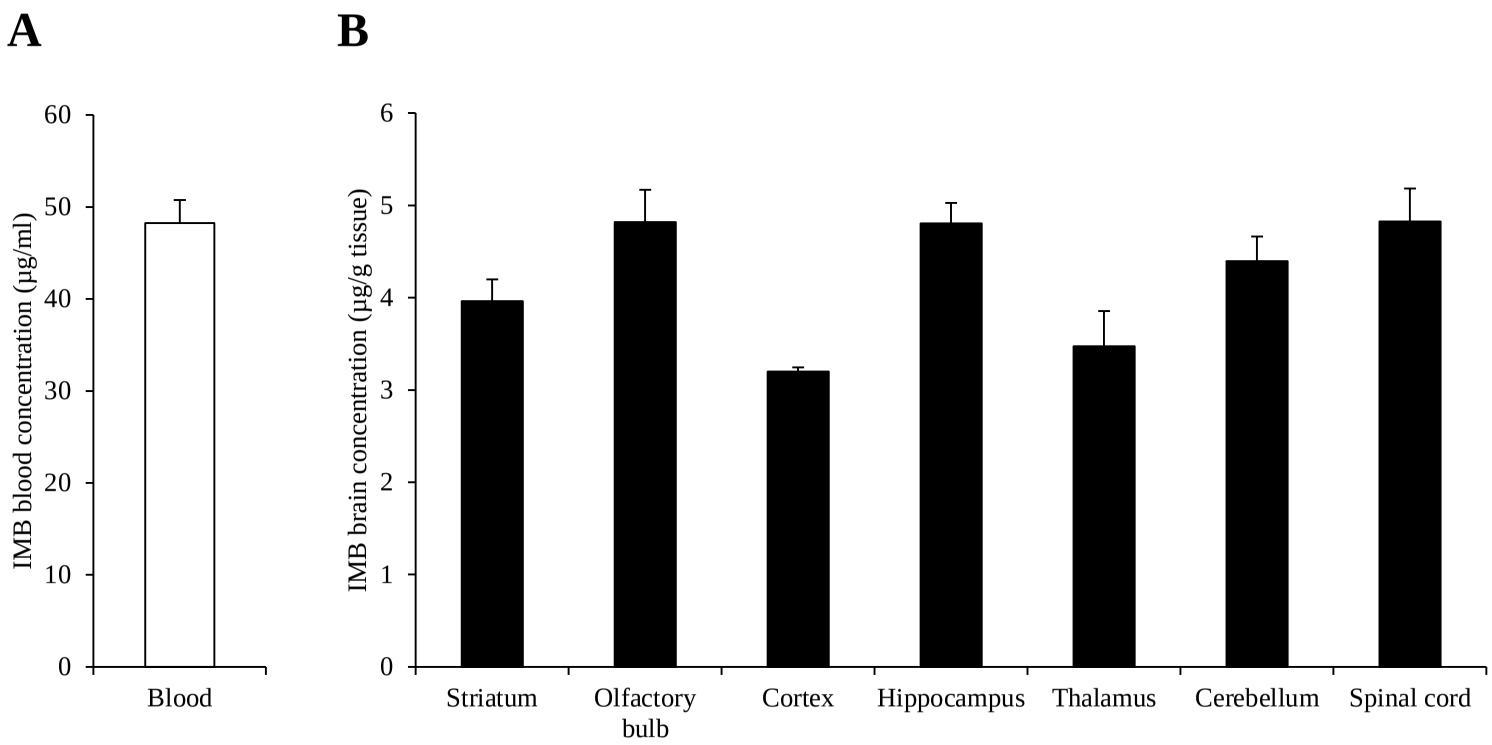

Figure 1. HPLC quantification of peripherally administered imatinib in naïve mice. HPLC analysis was performed to quantify concentrations of imatinib in the blood (n = 5), striatum (n = 4), olfactory bulb (n = 4), cortex (n = 5), hippocampus (n = 4), thamalus (n = 4), cerebellum (n = 4), and spinal cord (n = 4) of naïve mice that received single i.p. injection of imatinib mesylate (25 mg/kg) 30 min before sacrifice. Values are expressed as means ± S.E.M.

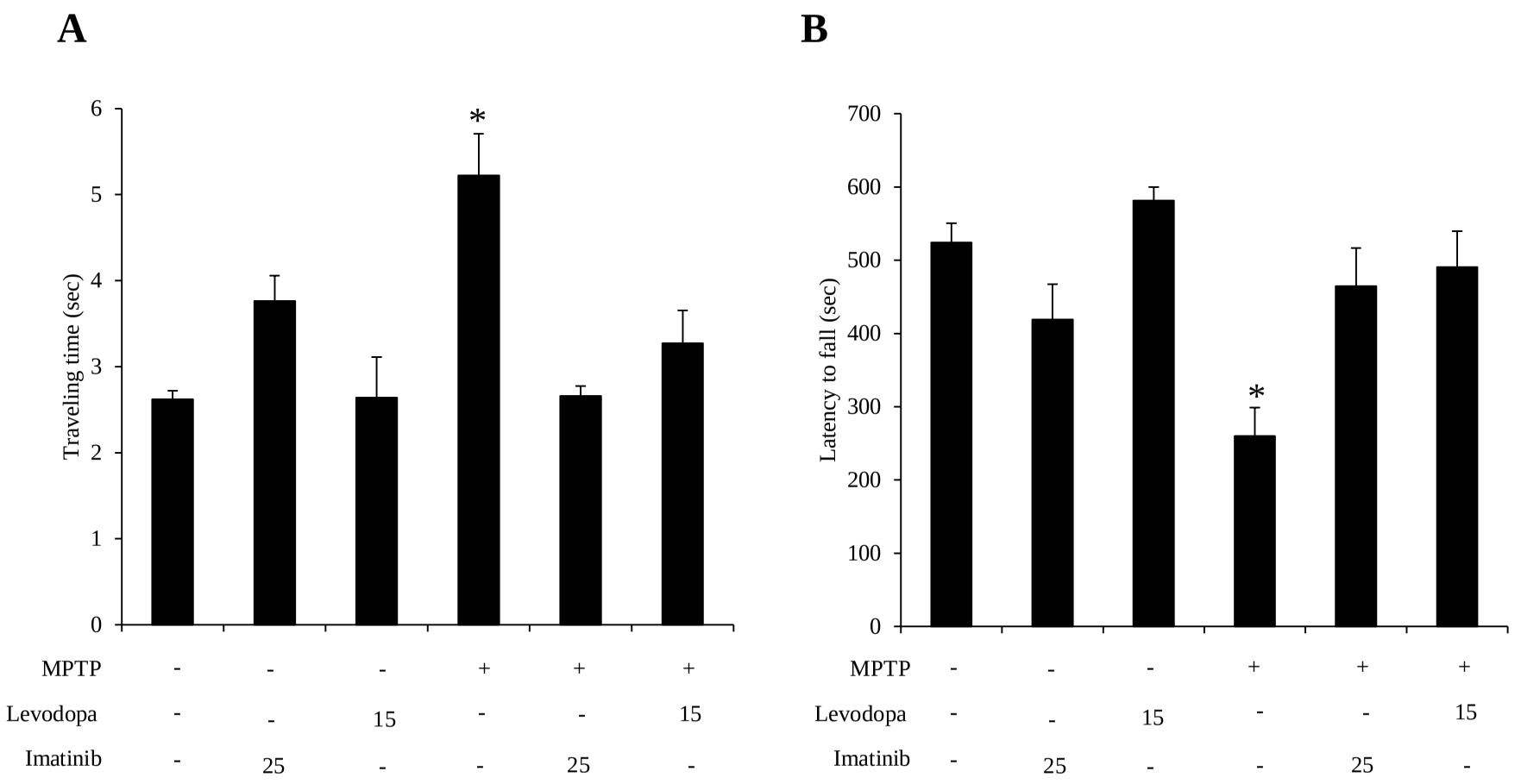

Figure 2. Symptomatic anti-parkinsonian effects of imatinib or levodopa in MPTP-treated mice. Behavioral tests were carried out in vehicle or MPTP-treated mice 30 min after single i.p. injection of imatinib or levodopa.
(A) The beam-walking test for examining the effects of administration of imatinib mesylate (25 mg/kg) or levodopa (15 mg/kg). Values are means ± S.E.M (n = 5-21). $^{*}P < 0.05$ versus vehicle-treated mice; one-way ANOVA [$F_{(5, 77)} = 11.265$] followed by the Scheffe *post-hoc* test.
(B) The rota-rod test for examining the effects of imatinib mesylate (25 mg/kg) or levodopa (15 mg/kg) administration. Values are means ± S.E.M (n = 8-21). $^{*}P < 0.05$ versus vehicle-treated mice; one-way ANOVA [$F_{(5, 80)} = 7.710$] followed by the Scheffe *post-hoc* test.

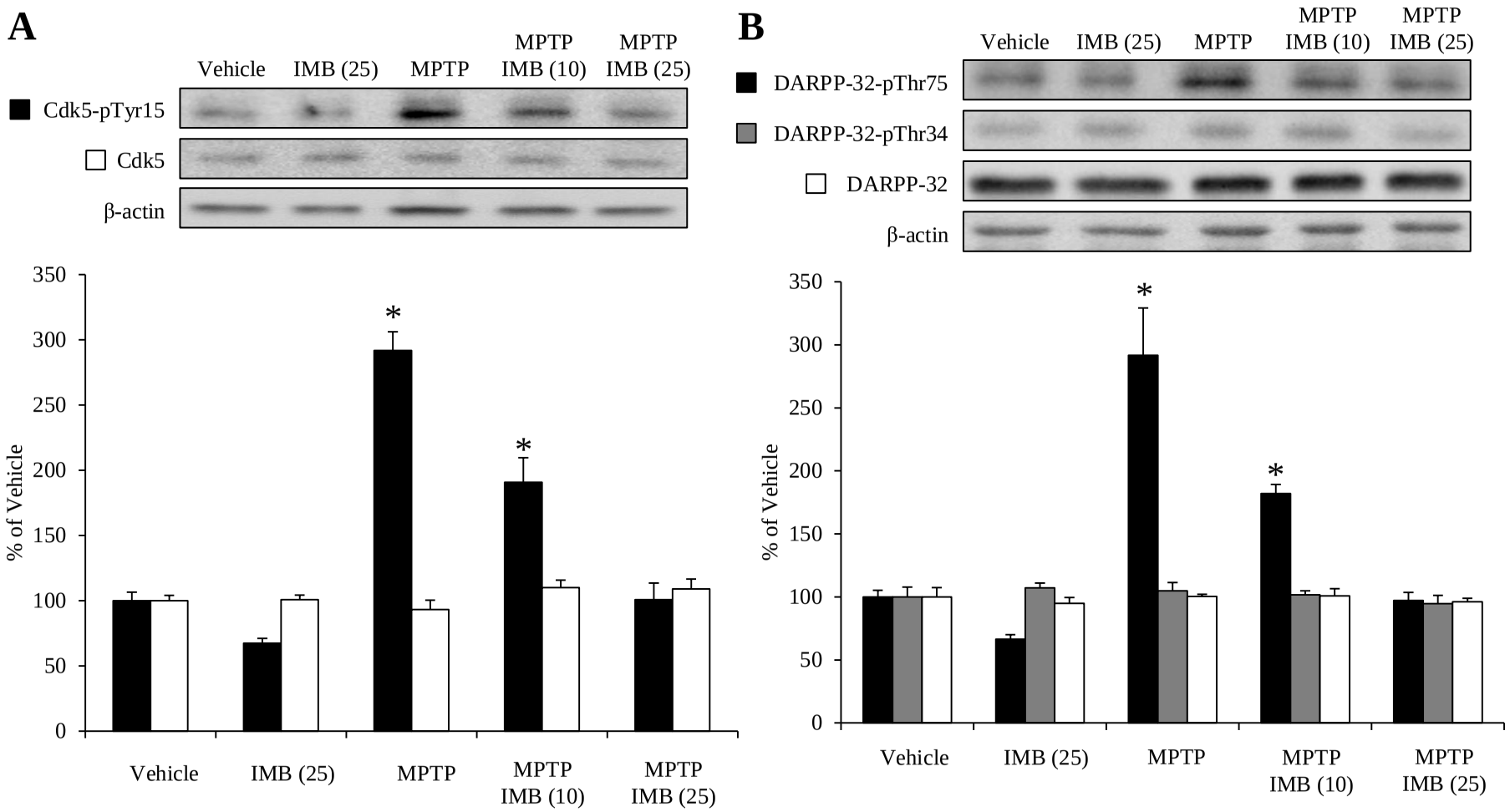

Figure 3. Western-blot analysis of the striatal levels of Cdk5-pTyr15, Cdk5, DARPP-32-pThr75, DARPP-32-pThr34, and DARPP-32 in vehicle or MPTP-treated mice 30 min after single i.p. injection of imatinib.

(A) Western-blot analysis of the striatal levels of Cdk5-pTyr15 and Cdk5. Values are means ± S.E.M (n = 4-5). $^{*}P < 0.05$ versus vehicle-treated mice; one-way ANOVA [$F_{\text{Cdk5-pTyr15 (4, 19)}} = 50.391$, $F_{\text{Cdk5 (4, 19)}} = 1.413$] followed by the Scheffe *post-hoc* test. IMB (10), imatinib mesylate (10 mg/kg); IMB (25), imatinib mesylate (25 mg/kg).

(B) Western-blot analysis of the striatal levels of DARPP-32-pThr75, DARPP-32-pThr34, and DARPP-32. Values are means ± S.E.M (n = 4-5). $^{*}P < 0.05$ versus vehicle-treated mice; one-way ANOVA [$F_{\text{DARPP-32-pThr75 (4, 19)}} = 35.089$, $F_{\text{DARPP-32-pThr34 (4, 19)}} = 0.711$, $F_{\text{DARPP-32 (4, 19)}} = 0.293$] followed by the Scheffe *post-hoc* test. IMB (10), imatinib mesylate (10 mg/kg); IMB (25), imatinib mesylate (25 mg/kg).

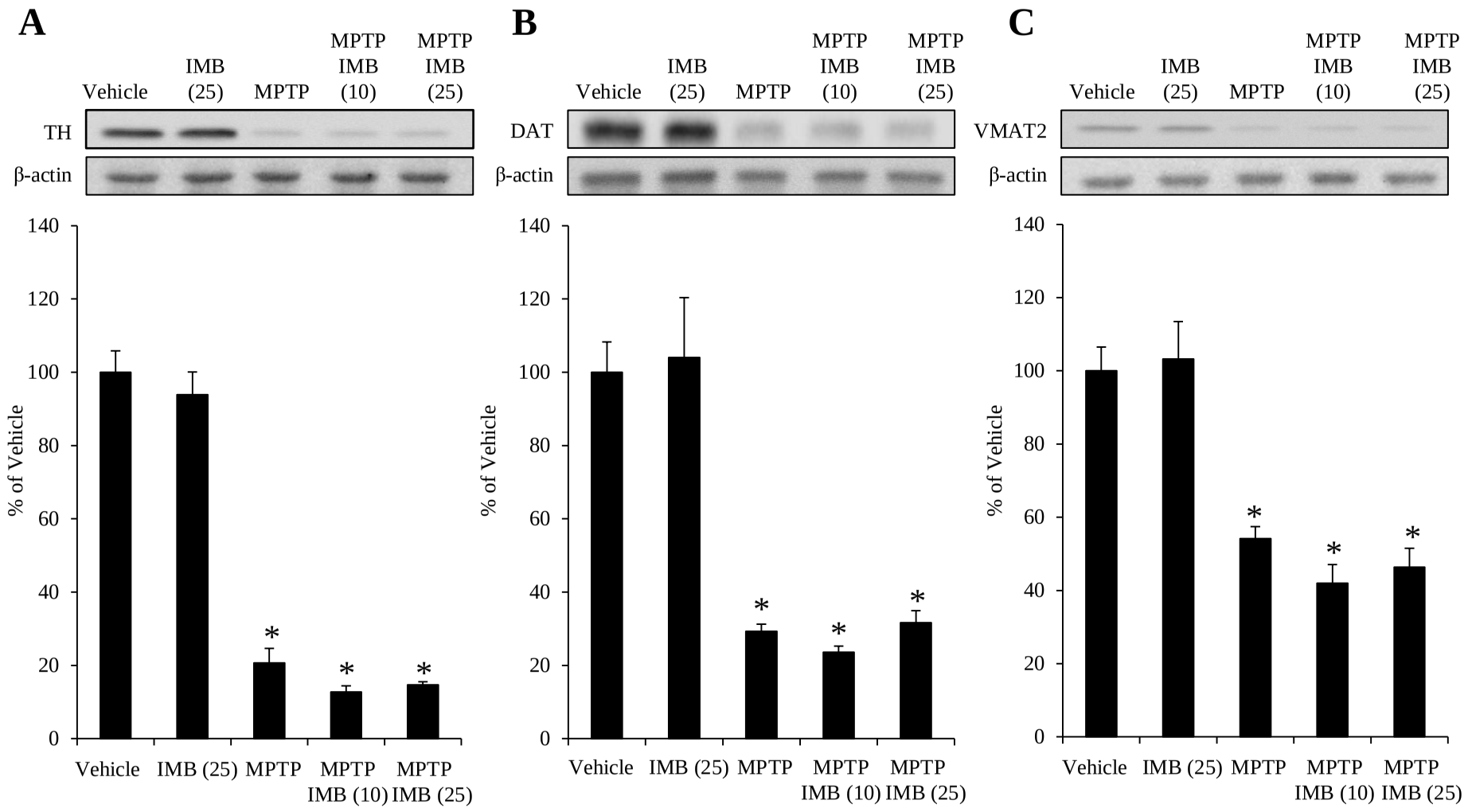

Figure 4. Effects of imatinib on striatal presynaptic dopaminergic markers in MPTP-treated mice. Western-blot analysis of striatal levels of TH, DAT, and VMAT2 were carried out from vehicle or MPTP-treated mice 30 min after single i.p. injection of imatinib mesylate (10 or 25 mg/kg). $^{*}P < 0.05$ versus vehicle-treated mice; one-way ANOVA [$F_{TH\ (4,\ 19)} = 107.43$, $F_{DAT\ (4,\ 19)} = 21.749$, $F_{VMAT2\ (4,\ 19)} = 20.615$] followed by the Scheffe *post-hoc* test. IMB (10), imatinib mesylate (10 mg/kg); IMB (25), imatinib mesylate (25 mg/kg).

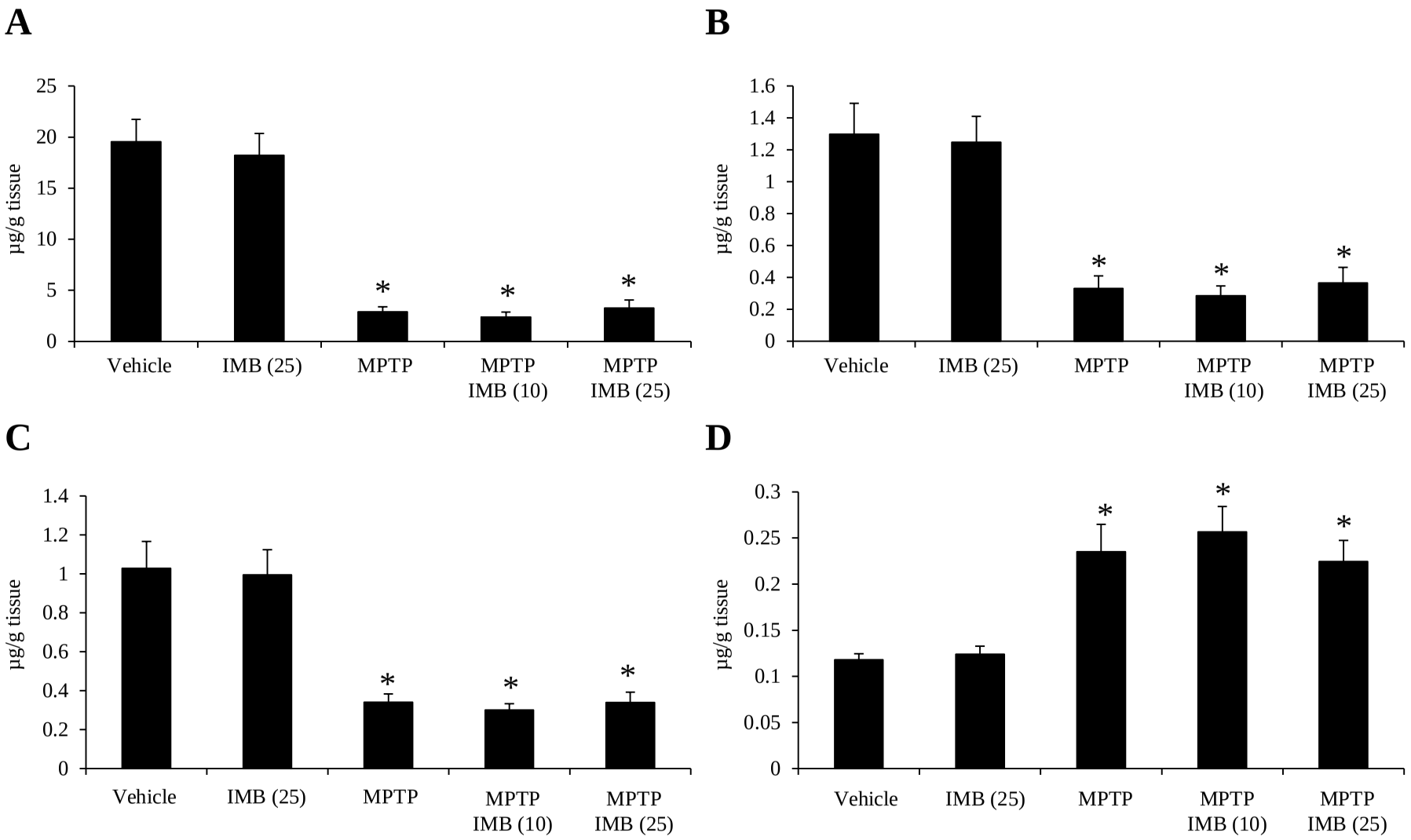

Figure 5. HPLC analysis of striatal levels of DA (A), DOPAC (B), HVA (C), and DA-turnover, which represents a net dopamine usage in striatum with (DOPAC + HVA)/DA (D). Values are expressed as means (µg/g tissue) ± S.E.M. (n = 4-5). *$P < 0.05$ versus vehicle-treated mice; one-way ANOVA [$F_{DA\ (4,\ 19)} = 34.526$, $F_{DOPAC\ (4,\ 19)} = 15.383$, $F_{HVA\ (4,\ 19)} = 16.078$, $F_{DA\text{-}turnover\ (4,\ 19)} = 10.355$] followed by the Scheffe *post-hoc* test. IMB (10), imatinib mesylate (10 mg/kg); IMB (25), imatinib mesylate (25 mg/kg).

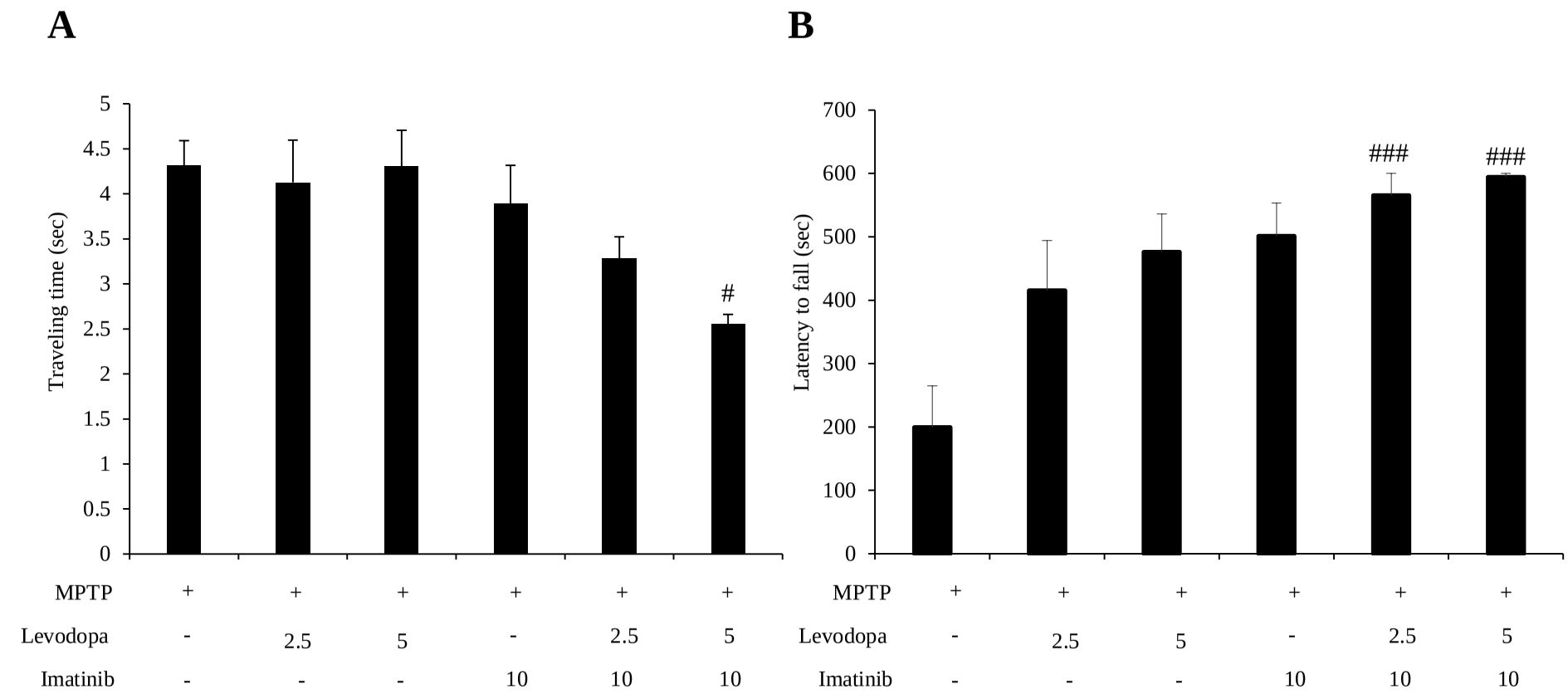

Figure 6. Symptomatic anti-parkinsonian effects with combining lower doses of imatinib and levodopa in MPTP-treated mice. Behavioral tests were carried out in vehicle or MPTP-treated mice 30 min after single i.p. injection of imatinib and/or levodopa.
(A) The beam-walking test for examining the effects of imatinib mesylate (10 mg/kg) and/or levodopa (2.5 or 5.0 mg/kg) administration. Values are means ± S.E.M (n = 10-11). $^{\#}P < 0.05$ versus MPTP-treated mice; one-way ANOVA [$F_{(5, 55)} = 4.177$] followed by the Scheffe *post-hoc* test.
(B) The rota-rod test for examining the effects of imatinib mesylate (10 mg/kg) and/or levodopa (2.5 or 5.0 mg/kg) administration. Values are means ± SEM (n =10-11). $^{\#\#\#}P < 0.001$ versus MPTP-treated mice group; one-way ANOVA [$F_{(5, 55)} = 8.283$] followed by the Scheffe *post-hoc* test.

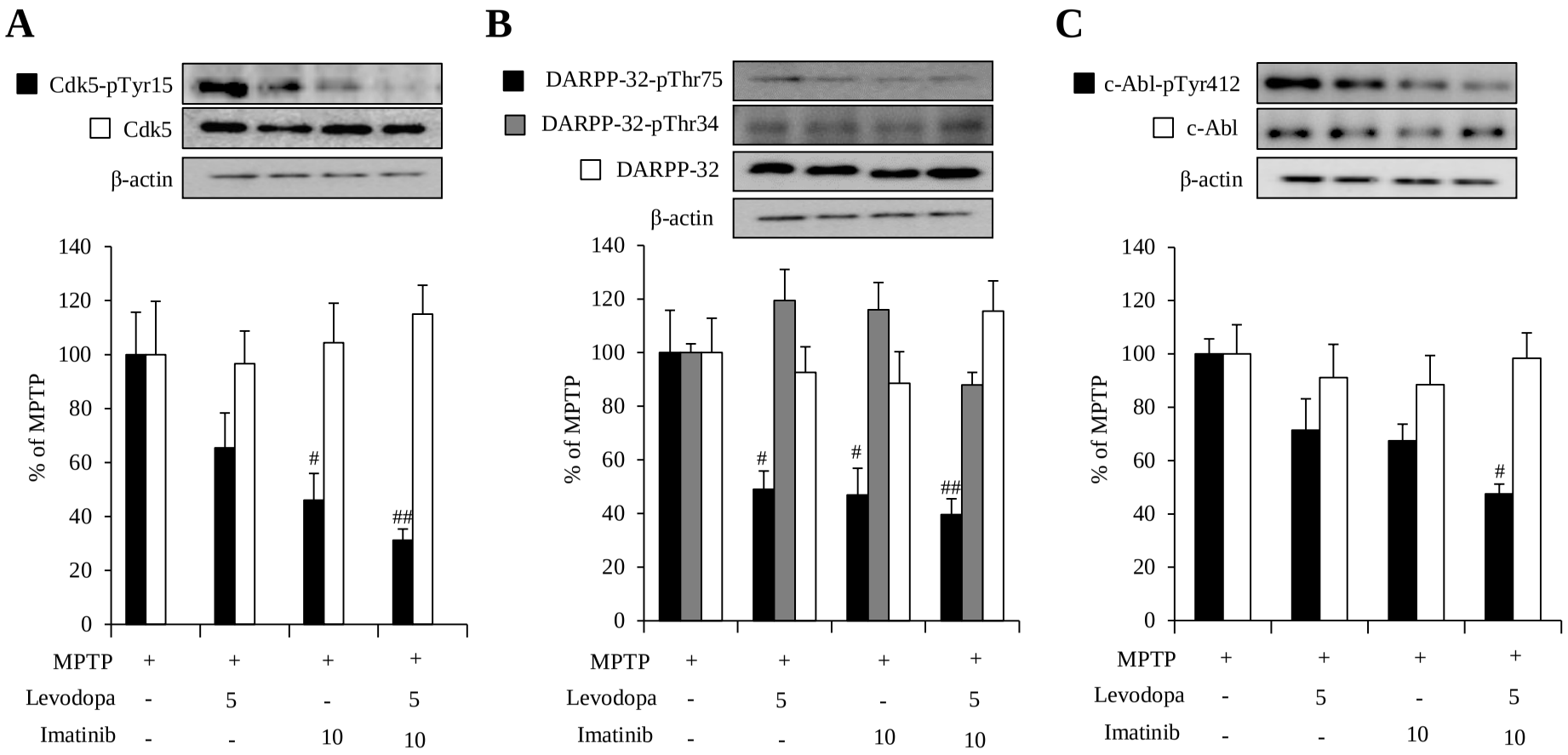

Figure 7. Western-blot analysis in MPTP-treated mice 30 min after single i.p. injection of imatinib and/or levodopa.
(A) Western-blot analysis of the striatal levels of Cdk5-pTyr15 and Cdk5. Values are expressed as means ± S.E.M. (n = 5-10). $^{\#}P < 0.05$ or $^{\#\#}P < 0.01$ versus MPTP-treated mice. One-way ANOVA [$F_{\text{Cdk5-pTyr15 (3, 31)}} = 6.039$, $F_{\text{Cdk5 (3, 17)}} = 0.258$] followed by the Scheffe *post-hoc* test.
(B) Western-blot analysis of the striatal levels of DARPP-32-pThr75, DARPP-32-pThr34, and DARPP-32. Values are expressed as means ± S.E.M. (n = 4-10). $^{\#}P < 0.05$ or $^{\#\#}P < 0.01$ versus MPTP-treated mice. One-way ANOVA [$F_{\text{DARPP-32-pThr75 (3, 29)}} = 5.529$, $F_{\text{DARPP-32-pThr34 (3, 16)}} = 1.257$, $F_{\text{DARPP-32 (3, 16)}} = 2.886$] followed by the Scheffe *post-hoc* test.
(C) Western-blot analysis of the striatal levels of c-Abl-pTyr412 and c-Abl. Values are expressed as means ± S.E.M. (n = 8-11). $^{\#}P < 0.05$ compared with MPTP-treated mice; One-way ANOVA [$F_{\text{c-Abl-pTyr412 (3, 34)}} = 5.820$, $F_{\text{c-Abl (3, 29)}} = 0.240$] followed by the Scheffe *post-hoc* test.

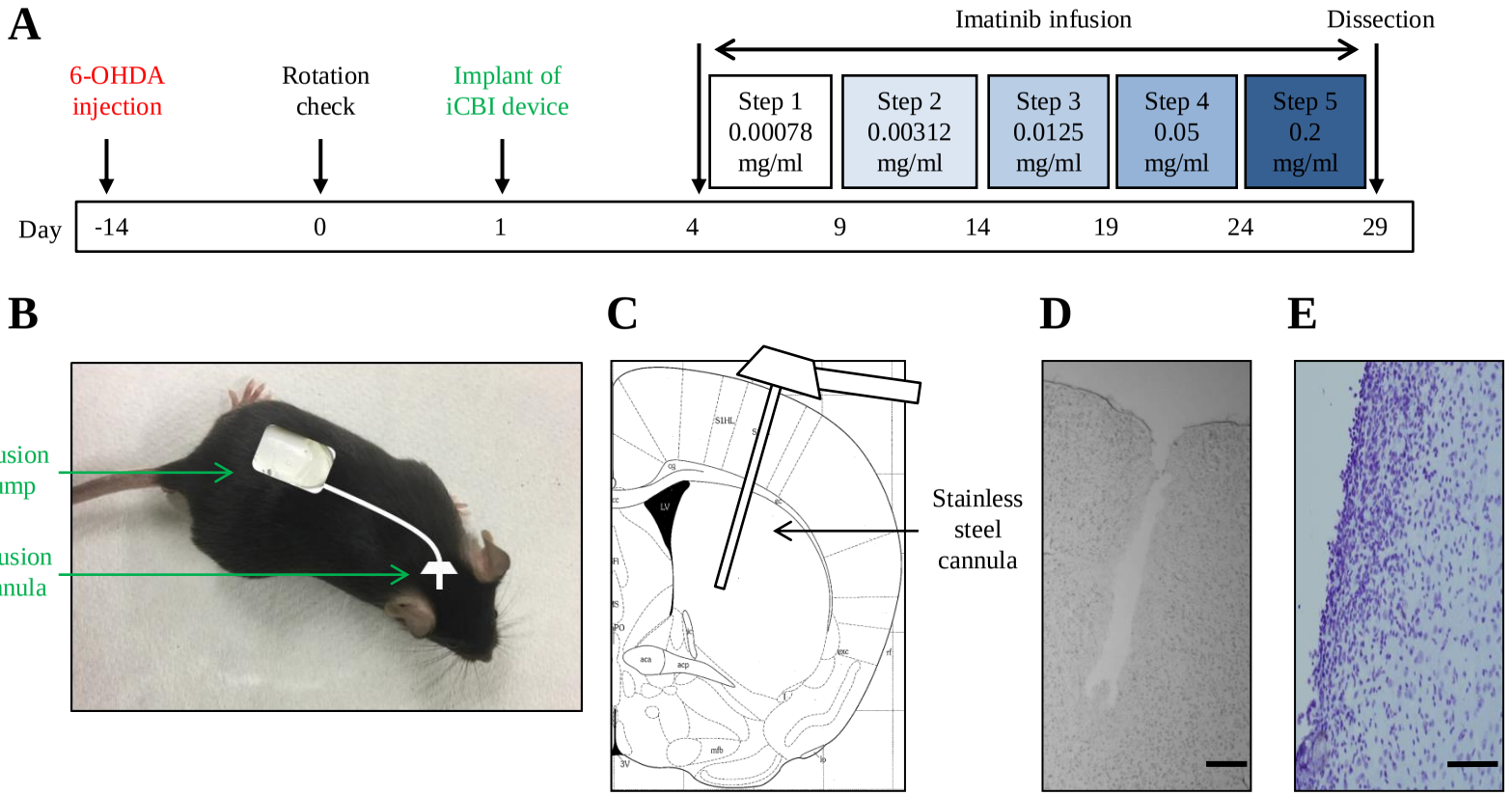

Figure 8. Experimental schedule and implant of the iCBI device with striatal tissue images in mice.
(A) 6-OHDA-lesioned mice were implanted with the iCBI device equipped with iPRECIO™ micro infusion pump. After a recovery of 3 days, mice received continuous intrastriatal infusion of imatinib mesylate 0.00078 mg/ml at a flow rate of 0.1 µl/h for the first 5 days (step 1), imatinib mesylate 0.00312 mg/ml at a flow rate of 0.1 µl/h for the next 5 days (step 2), imatinib mesylate 0.0125 mg/ml at a flow rate of 0.1 µl/h for the next 5 days (step 3), imatinib mesylate 0.05 mg/ml at a flow rate of 0.1 µl/h for the next 5 days (step 4), and imatinib mesylate 0.2 mg/ml at a flow rate of 0.1 µl/h for the last 5 days (step 5). In parallel, the PBS-infusion mice received 0.01 M PBS under the same protocol. At the end of infusion, mice were dissected and striatal tissues were used for western-blot analysis.
(B) The infusion pump and tubing connected with a stainless steel cannula were implanted under the skin, targeted into the right side of dopamine-depleted striatum of mice.
(C) A schematic image of the infusion cannula implanted into the right side of dopamine-depleted striatum.
(D) An optical microscopic image of the right side of striatum after fixation and removal of the cannula. Scale bar shows 0.5 mm.
(E) A Nissl staining image of the right side of striatum after fixation and removal of the cannula. Scale bar shows 100 µm.

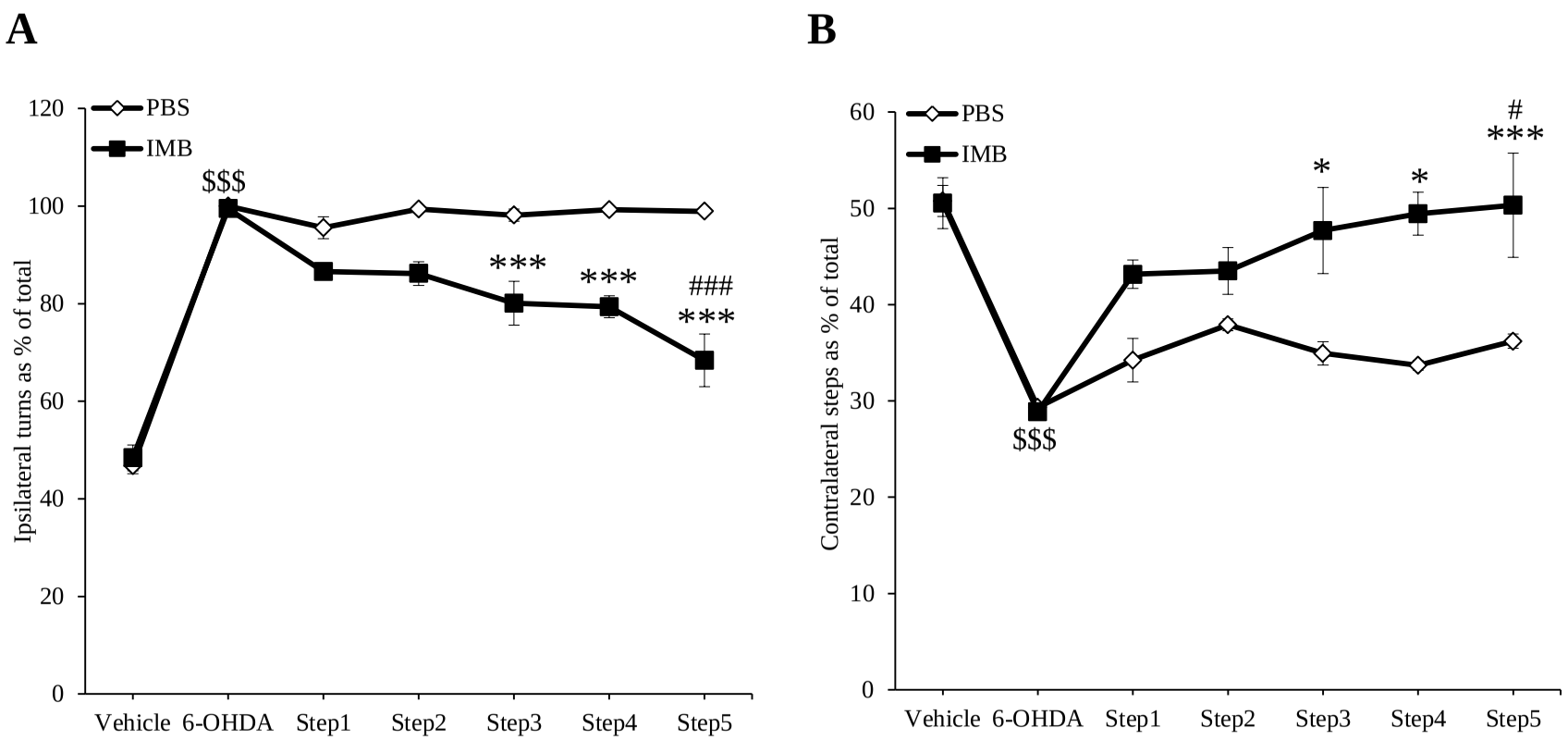

Figure 9. Symptomatic anti-parkinsonian effects of imatinib in 6-OHDA-lesioned mice. Spontaneous rotation and hind limb steps were analyzed after continuous intrastriatal infusion of imatinib.

(A) Spontaneous rotations ipsilateral to the 6-OHDA-lesioned side shown as % of total. $^{\$\$\$}p < 0.001$ compared with vehicle-treated mice; $^{***}p < 0.001$ compared with 6-OHDA-lesioned mice; $^{\#\#\#}p < 0.001$ compared with PBS control; two-way ANOVA ($F_{(group)\ 1} = 92.505$, $F_{(step)\ 6} = 103.491$, $F_{(group*step)\ 6,\ 72} = 11.331$) followed by Bonferroni *post-hoc* test. PBS, 0.01 M phosphate-buffered saline; IMB, imatinib mesylate.

(B) Spontaneous contralateral hind limb steps as % of total. Values are expressed as means ± S.E.M. (n = 5). $^{\$\$\$}p < 0.001$ compared with vehicle-treated mice; $^{*}p < 0.05$ or $^{***}p < 0.001$ compared with 6-OHDA-lesioned mice; $^{\#}p < 0.05$ compared with PBS control at step 5; two-way ANOVA ($F_{(group)\ 1} = 6.443$, $F_{(step)\ 6} = 5.947$, $F_{(group*step)\ 6,\ 48} = 1.613$) followed by Bonferroni *post-hoc* test. PBS, 0.01 M phosphate-buffered saline; IMB, imatinib mesylate.

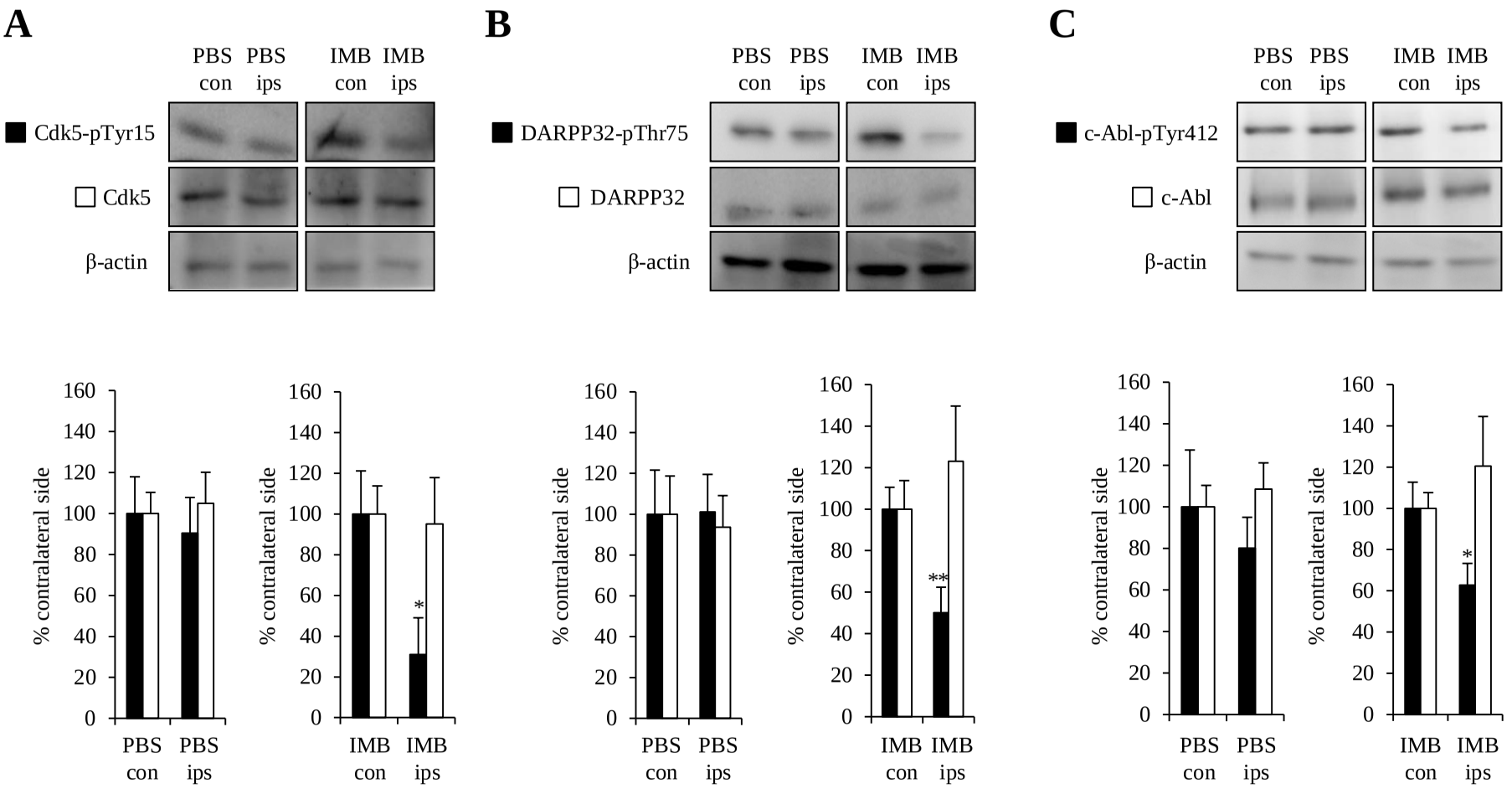

Figure 10. Western blot analysis in 6-OHDA-lesioned mice after continuous intrastriatal infusion of imatinib.
(A) Western-blot analysis of the striatal levels of Cdk5-pTyr15 and Cdk5. Values are expressed as means ± S.E.M. (n = 5-6). $^{*}p < 0.05$ followed by paired *t*-test. PBS, 0.01 M phosphate-buffered saline; IMB, imatinib mesylate; con, contralateral striatum; ips, ipsilateral striatum.
(B) Western-blot analysis of the striatal levels of DARPP-32-pThr75 and DARPP-32. Values are expressed as means ± S.E.M. (n = 5-6). $^{**}p < 0.01$ followed by paired *t*-test. PBS, 0.01 M phosphate-buffered saline; IMB, imatinib mesylate; con, contralateral striatum; ips, ipsilateral striatum.
(C) Western-blot analyses of the striatal levels of c-Abl-pTyr412 and c-Abl. Values are expressed as means ± S.E.M. (n = 5-7). $^{*}p < 0.05$ followed by paired *t*-test. PBS, 0.01 M phosphate-buffered saline; IMB, imatinib mesylate; con, contralateral striatum; ips, ipsilateral striatum.

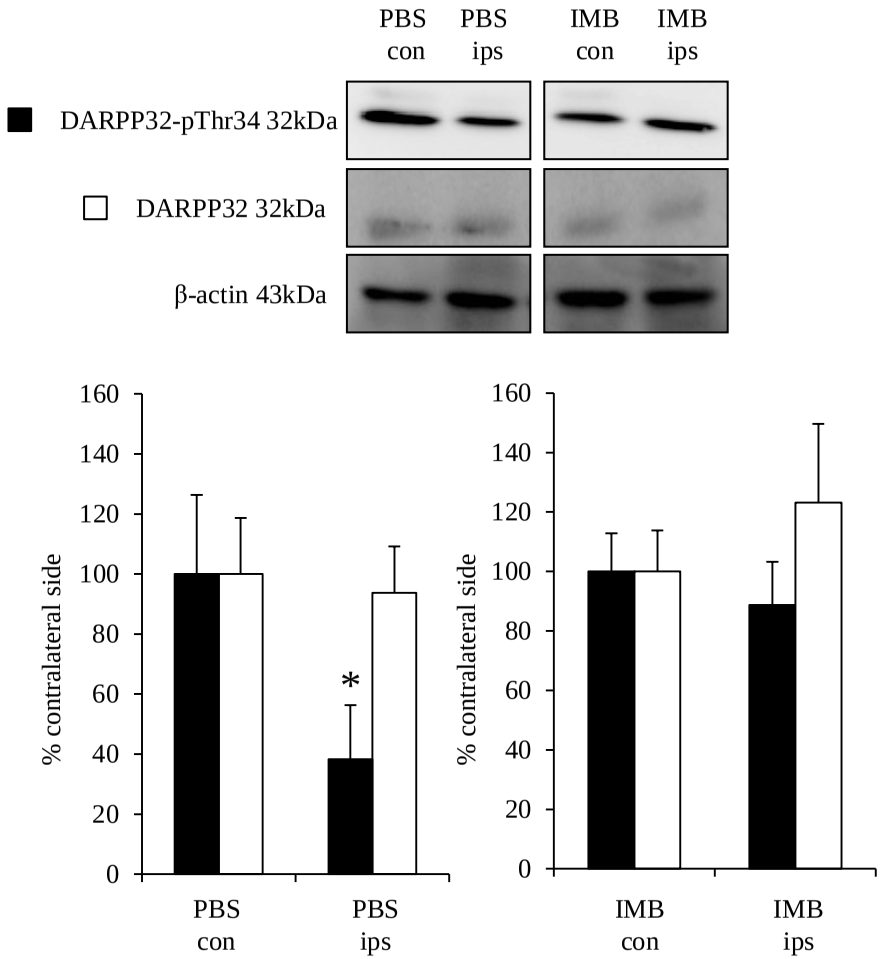

Figure 11. Western-blot analysis of the striatal level of DARPP-32-pThr34 in 6-OHDA-lesioned mice after continuous intrastriatal infusion of imatinib. Values are expressed as means ± S.E.M. (n = 6-7). $^{*}p < 0.05$ followed by paired *t*-test. PBS, 0.01 M phosphate-buffered saline; IMB, imatinib mesylate; con, contralateral striatum; ips, ipsilateral striatum.

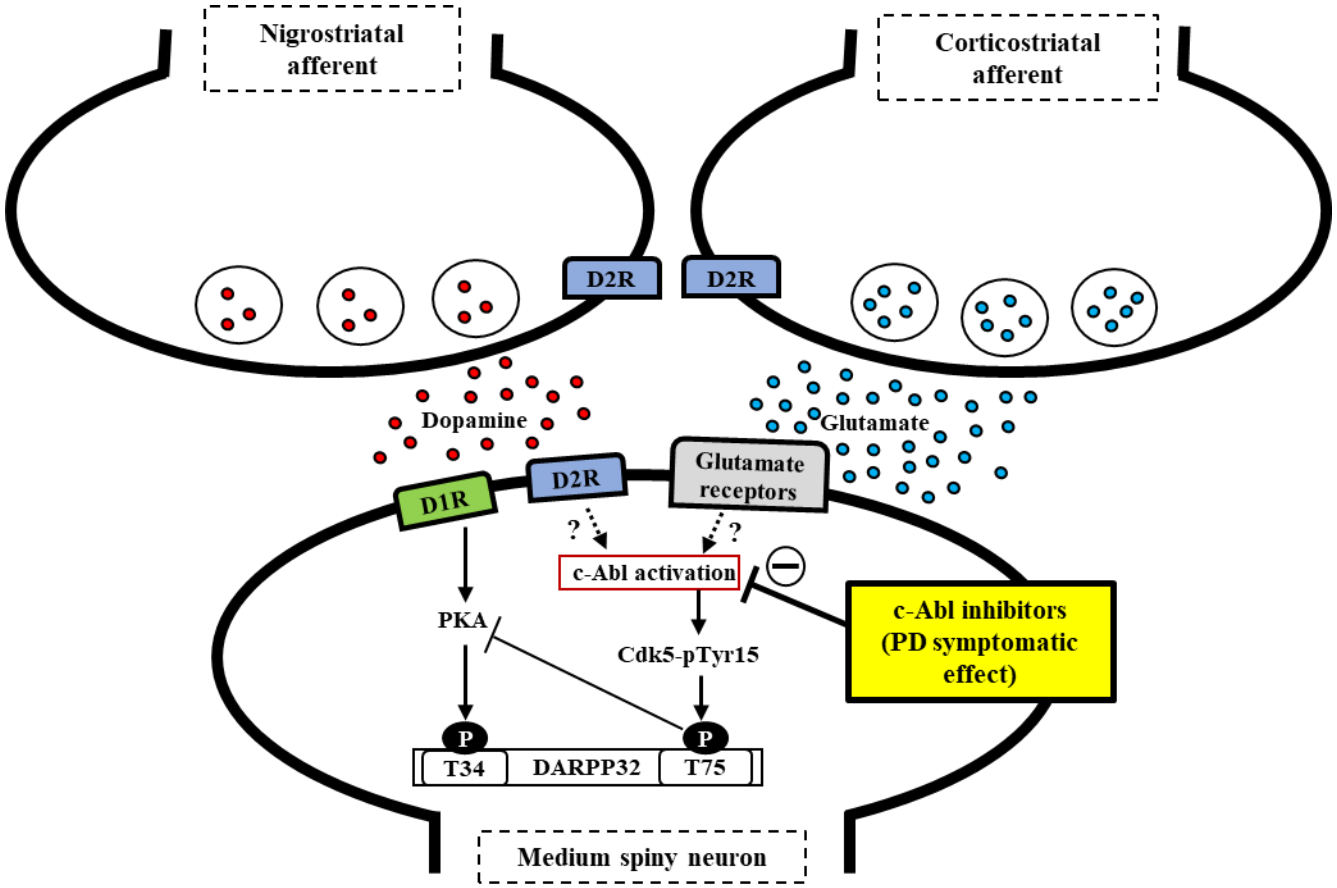

Figure 12. A hypothetical scheme showing symptomatic anti-parkinsonian effects of c-Abl inhibitors. Depicted are the possible roles of c-Abl inhibitors at postsynaptic level in the striatum. In the postsynaptic medium spiny neurons, dopamine deficiency may induce c-Abl activation to increase phosphorylation of Cdk5-pTyr15 and DARPP-32-pTyr75, resulting in an increased activity of the Cdk5/DARPP32-pThr75 pathway, which leads to parkinsonian symptoms. Thus, c-Abl inhibitors may exert symptomatic anti-parkinsonian effects at the postsynaptic level. PD, Parkinson's disease; D1R, D1-type dopamine receptor; D2R; D2-type dopamine receptor; Cdk5-pTyr15, Cdk5 with tyrosine 15 phosphorylation; T34, Threonine 34; T75, Threonine 75.